Precision Medicine Approach to Improving Reconstructive Surgery Outcomes for Breast Cancer Survivors

Katherine Emily Degen

Dissertation submitted to the faculty of the Virginia Polytechnic Institute and State University in partial fulfillment of the requirements for the degree of

Doctor of Philosophy
In
Biomedical Engineering

Robert G Gourdie
Kurtis E Moyer
Abby R Whittington
Mark Van Dyke
Steven Poelzing

April 20th 2018
Blacksburg, Virginia

Keywords: capsular contracture, wound healing, personalized medicine, artificial neural network, plastic surgery

Precision Medicine Approach to Improving Reconstructive Surgery Outcomes for Breast Cancer Survivors

Katherine Emily Degen

ABSTRACT

INTRODUCTION The single most common complication of reconstructive surgery requiring revision is the formation of a dense contractile scar capsule around the silicone implant called capsular contracture. Nearly all patients will experience this complication, though with different degrees of response, ranging from moderate scarring to major disfigurement and pain at the implant site. Presently, there is no way to predict the degree of contraction capsule formation that individual patients will suffer prospectively, nor is there clinical approach to preventing this complication.

METHODOLOGY Dr. Kurtis Moyer MD, Chief of Plastic Surgery at Carilion, provided patient samples of scar capsule and de-identified medical information under an active IRB. Standardization of collection was achieved by sampling scar capsule tissue, 1) from around an implanted breast expander device placed by Dr. Moyer, 2) at a standardized time interval following implantation of the device and 3) at a precisely defined anatomical location. Clinical data was collected for statistical analysis and tissue samples were prepared for histology and RNA-seq. Tissues were stained for αSMA, Vimentin, CCN1, CD68, CD86, CD163, CD31, Collagen I, Collagen III, and Collagen VI.

RESULTS A neural network model was created from the clinical data which predicts capsule severity. Analysis of the histology preparations demonstrated quantifiable differences between capsule grades. M1 macrophages were not different between grades while M2 macrophage density was inversely related to capsule grade and showed greater preference for the implant interface in the lower grade capsules. Myofibroblast density directly correlated to capsule grade and localized most densely just beyond the M2 high density region which was also rich in collagen VI.

RNA-seq was performed on a cohort of patients with asymmetric reconstruction results. A paired differential expression analysis resulted in 1029 significantly dysregulated genes. Of those, 189 had greater than one log fold change. Pathway enrichment was then performed which highlights IL4/13 signaling, extracellular matrix organization, antigen presentation, and interferon signaling as importantly dysregulated pathways. Differential expression results were also compared to various clinical and histological measurements to evaluate novel correlations. PVT-1, a long non-coding RNA oncogene, was strongly correlated to breast capsules formed after cancer removal. This suggests cancerous transformations of cell types that remain after the tumor is removed, such as cancer associated fibroblasts and macrophages.

CONCLUSION Capsule formation is a complex process but with well controlled clinical models quantitative differences can be found. These results serve as stepping stone for the field to move beyond retrospective clinical trials and pursue treatments and preventative measures.

Precision Medicine Approach to Improving Reconstructive Surgery Outcomes for Breast Cancer Survivors

Katherine Emily Degen

GENERAL AUDIENCE ABSTRACT

As the survival rate increases, the importance of quality of life post-cancer is increasing. This, in conjunction with genetic screening, has increase the number of breast reconstructions 36%. The most common complication causing revision of reconstructive surgery is the formation of a dense scar capsule around the silicone implant called capsular contracture. Nearly all patients will experience this complication, though with different degrees of response, ranging from moderate scarring to major disfigurement and pain at the implant site. Presently, there is no way to predict the degree of contraction capsule formation that individual patients will suffer prospectively, nor is there clinical approach to preventing this complication. Patient information and tissue was collected in a uniform manner to address these lingering problems. Clinical data was used to construct a predictive model which can accurately predict capsular contracture severity in breast reconstruction patients. Histological analysis demonstrated differences in structure and cell composition between different capsule severities. Of particular note, a new region was described which could serve as the communication interface between innate immune cells and fibroblasts. RNA-seq analysis identified 1029 significantly dysregulated genes in severe capsules. Pathway enrichment was then performed which highlights IL4/13 signaling, extracellular matrix organization, antigen presentation, and interferon signaling as importantly dysregulated pathways. These RNA results were also compared to various clinical and histological measurements to evaluate novel correlations. PVT-1, a long non-coding RNA associated with cancer, was strongly correlated to capsules formed after cancer removal. This suggests cancerous transformations of cell types that remain after the tumor is removed. Furthermore, transgelin and caspase 7 correlated to myofibroblasts density, suggesting an abnormal fibroblasts that are resistant to cell death and may have enhanced contractile abilities. Capsule formation is a complex process however, with well controlled clinical models quantitative differences can be found. These results serve as stepping stone for the field to move beyond retrospective clinical trials and pursue treatments and preventative measures.

Dedication

Deanna Kunkel & Peggy Randle

Acknowledgements

"Today is my one hundred and eleventh birthday!"

"Alas, eleventy-one years is far too short a time to live among such excellent and admirable hobbits." [cheers abound.] "I don't know half of you half as well as I should like, and I like less than half of you half as well as you deserve."

Tolkien, *The Lord of the Rings: Fellowship of the Ring*

Perhaps every PhD feels like it takes 111 years to complete. Regardless, it was a long journey not made by me alone. To my fellowship, thank you from the bottom of my heart. I would not have made it here without you.

"I regret to announce - this is The End. I am going now.
I bid you all a very fond farewell."

TABLE OF CONTENTS

TABLE OF FIGURES

LIST OF TABLES

CHAPTER 1: INTRODUCTION

Humans have utilized implants for as long as 7000 years, beginning with dental implants in ancient Egypt and Ireland.[1] This craft has been judiciously honed such that current implant functions range from dental implants to replacement joints and lenses, pacemakers and breast implants. The major limitation in developing implants is teaching the body to accept these implants. In the case of internal implant placement, the immune system responds as it would to a natural pathogen. For materials that degrade, the immune response continues until the material is completely degraded, whereas non-degradable materials elicit an immune response until it is walled off in a scar capsule. This prevents the threat from continuing to interact with the body and is reminiscent of the response to gram-negative bacteria.[2] In the case of implants, the reaction of the body is often detrimental to function by limiting mechanical coupling of device to tissue, in the case of joints, or by insulating electrical conduction in the case of pacemakers. In the case of breast reconstructive implants this response can result in a variety of complications including capsular contracture.

1.1 Overview of Capsular Contracture Literature

1.1.1 Clinical Importance

A clinical example of the foreign body response occurs following breast reconstruction with silicone implants. Aside from cosmetic breast augmentation, reconstruction post mastectomy is the most common reason for implant placement. As the 5 and 10 year survival rates for this cancer continue to improve, the demand for breast reconstruction has increased 39%.[3] Similarly, of patients who do not have breast cancer, but undergo mastectomies due to family history and/or encoding gene variants predictive of increased risk, many (~90%) opt for immediate reconstruction, especially if they are under 40.[4] The battle with breast cancer often leaves patients with a sense of identity loss even after successful treatment and patients see reconstruction as a pathway back to normalcy.[5,6] These factors in combination with a reconstruction awareness campaign launched in 2012

by the American Society of Plastic Surgeons are likely to continue to increase demand for reconstruction.

After a mastectomy, two reconstructive approaches are available; tissue expander or implant based (TE/I) or autologous abdominal tissue (AAT).[7] Despite a great deal of lingering worry associated with implant safety[8] their use is still popular. This number is likely to continue increasing because in 2012, the American Society of Plastic Surgeons launched a multi-year awareness campaign in order to inform patients of their options for reconstruction.[9] Despite some evidence that AAT provides better long term patient satisfaction, TE/I reconstructions constituted 83% of all reconstructions in 2010.[10] This prevalence necessitates conscientious effort to improve outcomes and control adverse events associated with an excessive foreign body reaction.[11]

Implant reconstructions can occur in one or two-stage reconstructions. One-stage procedures are now largely obsolete in the case of reconstructions as the immediate placement of a heavy implant causes a higher risk of implant failure. Two-stage reconstructions require the placement of a temporary silicone shell expander, most commonly at the time of mastectomy. The expander is slowly inflated with saline to gradually stretch the overlying skin and acclimate the tissue to the implant weight.[12] TE/I reconstructions experience several adverse outcomes including implant rupture, extrusion, infection and capsular contracture. Implant rupture has largely been addressed by changes in the material properties of the shell and silicone gel filling.[7,12] Extrusion occurs in 0.25 - 8.3% of cases with common causes being irradiation, compromised circulation to tissue covering the implants, and infection.[7,13] The most common problem requiring revision in implant reconstruction, is capsular contracture.[14]

Capsular contracture is a foreign body reaction that has a reported incidence between 3 and 50%. [7,12,15–17] The scar tissue surrounding the implant begins to contract and distort the implant shape and in some instances cause pain. Clinically, contracture is graded from I to IV on the Baker scale, with III and IV being the most severe grades. It should be noted that a grading of IV is based the presence of pain, and thus, the degree of contraction and resulting breast distortion may be less than that of any given grade. The etiology of severe

contracture is largely unknown; however, certain risk factors, such as radiation and smoking, have been well correlated to poor reconstruction outcomes and capsular contracture severity.[18–23] Interestingly, depression was recently linked to increased incidence of severe capsular contracture.[24] Independent of these factors, roughly 10% of individuals develop severe capsular contracture with no obvious cause.

Several causes for severe capsular contracture have been postulated. Large studies have been performed to correlate all manner of clinical factors with capsule grade; yet, few studies agree on any particular set of risk factors.[17,19,20,22,25] One theory that has gained traction recently is the importance of bacterial biofilms.[26–29] Agnello et al evaluated ten studies, including animal and human studies, concluding that biofilms were associated with more severe capsular contracture, especially those derived from Staphylococus epidermidis and Propionibacterium acnes. Both species are gram-positive bacteria common on the skin and could be easily introduced during surgery.[26] Limitations to this theory so far have been small sample size and introduction of biases by selecting patients who are electively having their implants removed. Additionally, the methods of testing for contamination vary in their sensitivity, likely contributing variation in study results.[27] Further work is necessary to test this theory.

1.1.2 Highlights of Capsular Contracture Literature

Many studies have looked at the structure and cellular populations in capsule tissue in an effort to understand the pathology. Hwang et al investigated the relationship of myofibroblasts numbers and tensile strength of capsule tissue to capsule grade. Both factors positively correlated to capsule grade, but only tensile strength was significantly correlated. They concluded that the number of myofibroblasts did not correlate to capsule grade; however, the large variability in the patient population could have limited their ability to detect an effect.[30] Despite this limitation, the correlation of tensile strength with capsule grade suggests there are structural differences in the matrix that are affecting the mechanical properties of the tissue. In support of this, collagen maturity has been reported to vary with capsule grade.[31] These findings are interesting and have potential implications for micro-behaviors driving capsule formation at the macroscopic level. How extracellular

matrix (ECM)-generating cells collectively orient and migrate in the tissue, as well as their inherent contractile properties may be important considerations. Such fibroblast-driven behaviors are likely downstream of initiating events in capsule formation and immune response.

Wolfram et al noted a large T cell infiltrate in grade III and IV capsules, but did not evaluate low-grade capsules for comparison.[32] Joseph et al investigated the time course of inflammation around implants in rats. Their results confirmed a large $CD4^+$ infiltrate that persisted at least until 180 days. Other work has attempted to elucidate the immune cell profile in capsule tissue. This work has been complicated because capsules removed from implant exchange procedures vary considerably in implant residing time and demonstrate a mostly resolved immune profile.[33–36] Wolfram followed up this work by describing a Th1/Th17 weighted t-cell response that resulted in fibrosis through a failure of regulatory T cells.[37]

It is possible that different patients show intrinsically different propensities for robust foreign body responses. Kyle et al have taken strides to support this hypothesis. In a microarray analysis of exchanged implant capsules, they found TIMP4 and IL-8 to vary significantly between low and high grade capsules.[33] Later work isolated fibroblasts from different grade capsules and assessed their contractile capabilities. Inflammatory markers were dysregulated between high and low capsule grades and fibroblasts from contracted capsules demonstrated greater contraction of collagen gels than normal breast fibroblasts. Additionally, conditioned media from the capsule derived fibroblasts was able to increase contractile abilities of normal fibroblasts.[38] These studies indicate that fibroblasts from more severe capsules maintain phenotype in culture and demonstrate different behaviors from non-contracted capsule (i.e., less severe) fibroblasts. It is unclear if these maintained phenotypic differences represent an intrinsic genetic difference in the differentiation potential of fibroblasts from different patients or if it results from the vagaries of inputs from external factors that may occur for a given surgery and/or a given patient or indeed as is likely, a combination of intrinsic and environmental influences.

1.2 Overview of Capsule Immunology

The immune response to foreign bodies has been well studied for a variety of materials in order to design better implants and improve patient standard-of-care. Model systems have been helpful in the study of the time course of the foreign body response. As raised earlier, animal models do not contract the capsule tissue around an implant. Because of this, thickness of the fibrous capsule is often seen as an output variable, less capsule equals a better implant. Interestingly, the robustness of this fibrotic response varies widely between individual humans, but not in standard research animal models. This species difference has limited studies on the underlying mechanism driving more severe contracture fibrosis in human patients. Many aspects of the foreign body response are conserved across scenarios, with surface chemistry being thought to be a key mediator of difference.[39–41] In general, serum and complement proteins rapidly adsorb to the implant surface after its placement. Macrophages and neutrophils arrive next to disinfect and clear debris. When the implant can't be broken down or extruded, macrophages begin to fuse. [2,42] The cascade of immune events that ensue generates the environment in which fibroblasts begin to build the capsule. [43,44]

Macrophages are outfitted with a wide variety of receptors that allow them to distinguish between self and non-self materials and appropriately dispose of them, including toll-like receptors, mannose receptors, and scavenger receptors. In the case of implants, these receptors bind to serum proteins, which have adsorbed to the surface. [2] It has also been demonstrated that macrophages bind to foreign materials via integrin-mediated adhesive interactions.[2,45] Phagocytosis is the macrophage's main tool against foreign materials, though, particles greater that 100μm in diameter cannot be engulfed by a single macrophage. In an apparent strategy to deal with larger objects, macrophages can be induced to fuse by the cytokines IL4 and 13, forming foreign body giant cells (FBGC) - doing so by utilizing cell membrane mannose receptors.[46–48]

All macrophages share phagocytic and antigen presenting capabilities to some degree however, their specific involvement in fibrosis is determined by two main phenotypes;

classical (M1) and alternative activation (M2).[47] The M2 phenotype is further divided into three sub categories (M2a,b, or c), each thought to have differing roles within the body, in some instances M1 is also split into a and b subtypes. [49] Classically activated macrophages are primed with interferon gamma (IFN-γ) and activated by pathogen signals such as lipopolysaccharide (LPS). [50] These cells secrete TNF, IL-12, IL-1 and IL-6 and are often marked with High CD86 expression and low mannose receptor expression. [50,51] On the other hand, IL-4 and 13 generated in a type 2 T helper cell (Th2) response can stimulate an M2 phenotype.[52] More specifically, M2a cells are activated by IL-4 and 13, M2b cells are stimulated by IL-1β or LPS in conjunction with immune complexes, and M2c cells are stimulated by IL-10 TGF-β or glucocorticoids. [53] It is important to note that while these cells are presented as distinct populations, they are by no means locked into a set phenotype. Stout et al demonstrated macrophages are plastic and highly sensitive to the microenvironment. [54–56] Initial responders to injury tend to be of M1 phenotype, which are responsible for cleaning the wound; while M2 cells seem to arrive or develop later and orchestrate resolution of inflammation.

T cells are white blood cells that mature in the thymus and are distinguished by the expression of T cell receptor (TCR). Their role in the foreign body response lies upstream of macrophages such that they can influence the macrophage phenotypes present in the response.[46] These cells can develop into a number of subtypes based on the environment that activates them. CD4 and CD8 are important markers, with CD8 cells being a marker for cytotoxic lymphocytes that deal with viral infections. $CD4^+$ cells are known as helper cells, as they assist in the activation of B-cells. $CD4^+$ cells are also divided into sub-classes. Type 1 T helper cells (Th1) that express IL-2 and IFN-γ and are induced by an exposure to IL-12 and IFN-γ, which activates the T-Bet transcription factor. Th2 produce IL-4 and 5 and are induced by IL-4 and the GATA4 transcription factor. Both cell types provide positive feedback, recruiting more cells of the same type, which allows T cell responses to become polarized. [46] Other sub classes of T cell have been described such as T regulatory helper (T-reg) and T helper 17 (Th17) cells. One study showed that T-regs inversely correlated with capsule grade[37], but little work has been done to evaluate the role of these cells in the foreign body response.[57–59]

Th1 cells induce macrophage activation and enhance their ability to phagocytose and kill pathogens. Macrophages in turn produce INF-γ and induce Th1 differentiation. Because of this feed-forward mechanism, there is a bystander effect where host cells are damaged by pathogen killing products of the macrophages. Th2 cells produce a number of inhibitory cytokines to prevent excessive damage. On the other hand, if the response becomes Th1 polarized, tissue damage can go unchecked. Th2 cells are cytokine factories that produce IL4, 10, 13 that induce M2 phenotypes. [53,60] Th2 cells are also responsible for the activation of pathogen-specific B-cells. [46] Because of these characteristics, a Th2-weighted response is generally considered a more favorable outcome for implant success, because it favors encapsulation and resolution of inflammation.

1.3 Fibroblasts and Capsule Construction

Fibroblasts, a largely mesenchymal cell type, are found in every tissue and are largely responsible for extracellular matrix deposition and maintenance. Fibroblasts can be identified by an abundant rough endoplasmic reticulum with elongated cisternae and a prominent golgi body (further detail can be found in [61]). Fibroblasts in granulation tissue are typically derived from tissue resident cells that are actively involved in matrix production and maintenance. Additionally, a precursor, the fibrocyte, has been reported to occur in the circulation and is sometimes recruited to wound sites to supplement the fibroblast population. [62–64] That said, it is unclear what contribution these cells make to overall collagen production. [65,66]

Regardless of their source, fibroblasts are activated upon wounding to begin proliferating, then they migrate within the wound bed and contract the granulation tissue. In 1971, Gabbiani et al described a phenomenon in which fibroblasts took on characteristics of smooth muscle cells when activated by wounding, which was hypothesized as causal for contraction. [67] Now known as myofibroblasts, these cells are most commonly identified by alpha smooth muscle actin expression, which is believed to be important for the contractile phenotype. It was proposed that these activated fibroblasts were responsible for wound contraction. [68,69] However, this model is not universally accepted. Ehrlich et al utilized various wound healing models with and without vanadate, which blocks αSMA expression,

demonstrating that wound contraction was relatively undisturbed. Interestingly, collagen bundles of vanadate treated models were thicker and more aligned than controls, which also increased the tensile breaking strength of the scar tissue. [70–72] Moreover, wounds treated with SB505124, a TGF-β inhibitor, showed no myofibroblasts, but contracted normally.[73] Gabbiani subsequently described myofibroblasts as a terminal differentiation along a continuum of phenotypes ranging from a traditional fibroblast to a smooth muscle cell. They proposed a two-step differentiation in which a cell type known as a proto-myofibroblast, in an intermediate stage between fibroblast and myofibroblasts, was capable of contraction, but did not yet express αSMA. [74] The progression of the immune response, discussed above, influences this activation and subsequent behavior of fibroblasts.

Most of what is known about fibroblast activity is derived from wound healing models that focus on skin. While the clot is established, local fibroblasts, or their progenitors, are proliferating at the wound edges. [75] Roughly 3 days after wounding fibroblasts begin to migrate into the wound and produce granulation tissue. [76] Fibroblasts tend to migrate individually, in contrast to epithelial cells which travel as a sheet, thus it is counter-intuitive that they should proliferate at the wound edge and then begin migrating en masse. It has been proposed that the high density build-up of fibroblasts helps to program these cells to behave differently once released to act individually.[77] How these cells move and interact with each other as they lay down matrix is fundamental to understanding the final scar structure and as it stands at present, this process is not well understood.

Migration of most cells consists of four basic sequential events: protrusion of the leading edge of the cell, adhesion to ECM, cell body movement, and retraction of the trailing edge. [78] In 2D culture ligand density, reminiscent of ECM, is critical in determining cell speed and direction.[79–81] Fibroblasts allowed to migrate without chemotactic or durotactic signals in culture have been shown to regulate their directionality via a Rac switch.[82,83] By decreasing Rac activity Petrie et al suppressed peripheral lamellae and switched the cell migration patterns of both fibroblasts and epithelial cells from random to directionally persistent movement. [83,84]

Migration in 3D structures has proven to be very different from 2D migration. For example, ligand density can reach an inhibitory level in 2D, whereas this phenomenon is not reported in 3D. [85,86] The most popular model for this work is the collagen gel contraction assay. In this model, cells are suspended in a collagen solution that then sets into a gel. Over time the fibroblasts reorganize the collagen matrix and contract the gel, thereby providing a semi-quantitative assay of fibroblast-mediated collagen contraction. Studies with this model have demonstrated that matrix stiffness is important to cell migration. If the matrix moves under cell-mediated traction force, the cell remains stationary, as on a treadmill, until the matrix is compacted. On the other hand, if the matrix fails to move under the influence of cellular traction, these forces can translate into movement of the cell body. [87] Doyle et al has proposed that cells in 3D matrices utilize 1D migratory mechanisms that are dependent on myosin II contractility and microtubules. [84] This was further supported by a study that showed cells offered a multilayer mesh interacted with a single plane at a time and only infrequently transitioned between planes.[48,88,89] While insightful, these studies focus on single cell movements, which leaves open important questions on how cells cooperate to generate larger scale structures- such as scar tissue. [77]

Fibroblasts begin remodeling granulation tissue by producing large quantities of collagen and other matrix proteins. [90,91] Because collagen self-assembles into fibrils *in vitro*, it was thought that fibroblast were little more than factories for this important molecule. Harris et al determined that fibroblasts generate tractional forces that far exceed what is needed for simple locomotion. These authors hypothesized that this excess force was generated for the organization of the fibroblasts' substrate i.e. the fibrillary collagen network.[92] The work of Stopak et al built on this hypothesis by demonstrating that exogenous fluorescent collagen injected into a developing limb bud was incorporated into tissues despite forming a gel minutes after injection. These findings suggest that an active mechanism is involved in organizing collagen and that the tractional forces of migrating cells are a key aspect of this mechanism.[93] These findings are further supported by Gunn et al who reported that fibroblasts utilize exogenous collagen to restore tendons when their own protein synthesis is inhibited. [94]

Many groups have since shown fibroblasts to be instrumental in the pattern of collagen being introduced into the scar. Meshel et al. showed that fibroblasts use α2β1 integrin to hold collagen with their lamellipodia and manipulate its position in what they described as a 'hand-over-hand' motion cycle. These workers also demonstrated that myosin II B was important for generating the force to move collagen fibers during the remodeling process.[95] Evidence from other groups has also supported a myosin-dependent mechanism of collagen translocation. [96] This being said, other studies have questioned this mechanism. Tamariz et al were unable to detect any association between the protrusion and retraction of cell extensions and collagen remodeling and could find no correlation between Rho kinase signaling and the translocation of collagen fibrils. [87]

Recent work by Castella and co-workers proposed a lock-step mechanism of contraction mediated by myofibroblasts/fibroblasts. In this model, strong Rho and ROCK-mediated isometric cell contraction was suggested to generate slack in individual collagen fibrils. These slack fibrils were then envisaged as being pulled in a ratchet-like mechanism by periodic $[Ca^{2+}]_i$-dependent microcontractions, until fibril tension was restored. Locally contracted fibrils were proposed to be enzymatically modified and/or stabilized by addition of new ECM material and new crosslinks. Once remodeled, the fibers were then proposed to be again available to generate mechanical load – with cells being able to re-lengthen while the ECM remained shortened. [97]

In addition to manipulating orientation, fibroblasts are also important in maturation of the ECM by compacting immature thin collagen fibrils into dense and mature fibers. Early work showed that this collagen packing requires the removal of water molecules between the fibers. It was later demonstrated that the cytoplasmic microfilaments pull collagen fibrils over the fibroblast's plasma membrane surface, bringing collagen fibrils in closer contact driven by myosin ATPase motor.[98] Cytoskeletal structures and focal adhesion formation have also been implicated as key to this process.[74,86,87,99] Canty et al demonstrated that disruption of microtubules slowed secretion but did not otherwise affect collagen. On the other hand, disassembly of the actin cytoskeleton decreased aligned organization of collagen fibrils in chick tendons.[100] Fibroblasts are highly sensitive to their mechanical environment through focal adhesions, which regulates not only migration and

cell shape but also protein production. [101–104] Additionally, focal adhesion size has been shown to regulate recruitment of α-SMA to stress fibers, which in turn regulates the amount of force that activated fibroblasts are able to generate.[105,106]

Fibroblasts also interact with numerous matrix and matricellular proteins that help instruct their activities. These proteins can stimulate the production of matrix proteins, alter cell migration, and themselves contribute to the mechanical properties of the tissue. Some of these molecules include fibronectin[107–110], fibrin[76,111], calreticulin[112,113], decorin[114,115], thrombospondin[116,117], and sparc[118–120]. While of great importance, the investigation of these proteins is currently beyond the scope of this introductory review.

To this point, research has been focused very tightly on the collagen/fibroblast interaction or the role of different molecules in structure. Little work has been done to evaluate the collaborative effort of fibroblasts in overall scar structure. It is unclear if a single fibroblast traverses a large area of the wound or if they remain localized. Each scenario would suggest very different levels of coordination and logical steps in the construction of the scar tissue.

1.4 Project Rationale

Capsular contracture is poorly understood at the mechanistic level. Key evidence suggests that capsule grades histologically differ in collagen structure[31] and immune response. [34,121] Very little has been evaluated in between these two extremes. Undoubtedly, the immune response generates the environment in which the collagen matrix is being built, but it is unclear if the degree of the immune response is sufficient to drive severe capsule formation. Little information is found in literature about the genetic influences on scarring; some candidates associated with keloid or hypertrophic scars include MHC alleles and TGF-β mutations.[122,123] Other work has implicated differential regulation of matrix remodeling enzymes as genetic differences in scar responses.[33]

Another aspect that has been poorly evaluated is why some capsules aggressively contract while others do not. Looking at end-stage capsules, after residing times of years, demonstrates the structure that is highly crosslinked to hold tension. Other work has demonstrated that higher grade capsules have higher tensile strength[30] but how capsule

tissue comes to organize in this manner is unclear. It is also unclear if there are differences earlier in capsule formation that would illuminate the mechanism that leads to greater contracture. Some work suggests that fibroblasts are more contractile in severe capsules[38]. Do fibroblasts show a genetic predisposition for greater contracture or are they programed to be that way by externally determined wound-to-wound variation (e.g., the occurrence of an infection) in the healing environment?

Studies thus far have been limited to elective removal of implants or rodent models, both of which fail to assess these important aspects of the pathology at relevant time points. Given the prevalence of two stage reconstructions, a new model is more accessible to researchers that can address the lack of control in previous clinical models, while maintaining human relevance. More rigorous evaluation of immunology, fibroblast behavior and tissue structure could provide clues to the etiology.

The work presented here aims to characterize capsular contracture with a highly standardized human model. *Chapter one* has covered what is known thus far from traditional studies of capsular contracture and the foreign body response. *Chapter two* presents a new clinical tool which predicts capsule severity for individuals based on clinical factors. *Chapter three* is an in depth quantification of capsule tissues derived from silicone shell expanders. This quantification identified a novel region in which the implant interface, rich with macrophages and collagen VI meets a band of tissue rich in activated fibroblasts. This region could serve as a priming area in which fibroblasts are programed for capsule deposition. *Chapter four* explores the application of RNA-seq to capsular contracture. By conducting a paired analysis of two capsule samples from asymmetric patients novel genes and pathways were identified for future exploration.

CHAPTER 2: Prediction of Capsular Contracture Severity Following Post-Mastectomy Reconstruction by a Neural Network Model

2.1 ABSTRACT:

Objective To develop a new tool that can reliably predict severity of capsular contracture in cancer patients undergoing breast reconstruction and assist physicians in evaluating potential for asymmetry, patient education of risk, and generating hypotheses for clinical management of capsular contracture.

Design Cohort study with artificial neural network analysis.

Setting Cohort information and tissue samples were collected at the Carilion Clinic in Roanoke, Virginia under IRB Protocol #1289. A novel approach was developed to limit variation, while maintaining a human model. This study utilized patients undergoing two-stage reconstruction following mastectomy, prophylactic or cancer treatment. By doing so, all capsule severities were evaluated at a uniform 3-4 month window as opposed to a large range of years, as in previous studies. Additionally, only a single implant and procedure type were utilized.

Main outcome measures Predictive accuracy of an artificial neural network trained on a subsample of our cohort.

Results A robust artificial neural network (ANN) was developed from a well-controlled 89 patient cohort. An ordinal logistic regression for grade was performed as a baseline for the construction of an ANN. The best fitting model was generated using 8 input variables, 2 hidden layers and both linear and hyperbolic tangent node equations. Including inputs describing blood flow and capsule thickness drastically improved model performance from a model containing cancer status, patient age, chemotherapy, radiation, diabetes and smoking (from R^2= 0.62, Misclassification Rate 28% to R^2 0.94, Misclassification rate 4.5%). Utilizing the larger model, predictions can be made about capsule grade based on their clinical data. Risk of asymmetry can be highlighted as well as the impact of lifestyle risk factors, diabetes and smoking on reconstruction outcome. Finally, this model suggests the importance of modulating capsule thickness and blood supply to the capsule as a potential treatment.

Conclusions This ANN reliably predicts capsule severity given patient's clinical characteristics which are readily available. It advocates for the importance of monitoring capsule thickness and blood flow via Doppler flow ultrasound. This model has potential to advise both patients and physicians of the risk of severe capsular contracture risk and can also provide hypotheses for interventions that might limit capsule severity.

2.2 INTRODUCTION

Breast cancer often leaves patients with a sense of identity loss even after successful treatment and patients see reconstructive surgery as a pathway back to normalcy.[5,6] As the 5 and 10 year survival rates for this cancer continue to improve, the demand for breast reconstruction has increased 39%[3]. Similarly, of patients who do not have breast cancer, but undergo mastectomies due to family history and/or encoding gene variants predictive of increased risk, many (~90%) opt for immediate reconstruction, especially if they are under 40.[4] The most common cause of revision in patients undergoing breast reconstruction is capsular contracture, a foreign body reaction that has a reported incidence between 3 and 50% [7,12,15–17]. In capsular contracture the scar tissue surrounding the implant contracts and distorts implant shape, and in some instances causes pain. Clinically, capsular contracture is graded from I to IV on the Baker scale, with III and IV being the most severe grades. [124]

After a mastectomy, two reconstructive approaches are available; tissue expander or implant based (TE/I) or autologous abdominal tissue (AAT).[7] Although there is some evidence that AAT provides better long term patient satisfaction, TE/I reconstructions constituted 83% of all reconstructions in 2010.[10] This prevalence necessitates conscientious effort to improve outcomes and control adverse events associated with an excessive foreign body reaction.[11] Unfortunately, the etiology of severe contracture is largely unknown. Certain risk factors, such as radiation and smoking, have been correlated to poor reconstruction outcomes and capsular contracture severity.[18–23,125] Interestingly, depression was recently linked to increased incidence of severe capsular contracture.[24] Despite the size of previous studies, many correlative findings conflict, leaving physicians without a clear path to advising their patients of risks.

First designed in 1959, artificial neural networks (ANN) are a statistical approach that has received increasing attention for solving prediction and classification problems.[126,127] These models begin with a set of input variables, which are fed into a network of computational nodes. These nodes are organized in layers and act as non-linear summations. The connections between these nodes are given weights that are adjusted through training to optimize the output classification. Eftekhar and co-workers showed that ANN outperform logistic clinical models in discrimination and calibration and note they are robust in dealing with noisy or incomplete data.[128] Additionally, when

ANN was applied to psychological diagnosis and prediction of behavior outcomes such as suicide attempts, it outperformed regression models. It was noted as particularly valuable because of its empirical analysis, even when insufficient knowledge is available or existing knowledge is debated.[129] This method is ideally suited for the predictive problem of capsular contracture, which is potentially influenced by a complex set of environmental and genetic variables. The study described herein constitutes a novel application of neural network modelling to create a clinically relevant predictive tool.

2.3 METHODS

Patient Population

Patient information and clinical variables were collected from women undergoing breast reconstruction following mastectomy with approval of IRB Protocol #1289, presented in Table 2.1. A total of 89 capsules were included in this analysis (Table 2.1). Patients with known connective tissue disease or other diseases associated with abnormal wound healing were excluded. Additionally, histological data, including capsule thickness and vessel size, was collected (Figure 2.1).

	Grade I	Grade II	Grade III	Total
Patient Age	48.83 ± 14.1	48.05 ± 9.49	51.93 ± 13.3	49.51 ± 11.3
Residing Time	3.83 ± 1.2	4.17 ± 1.8	3.81 ± 1.2	4.02 ± 1.6
Cancer	50.0%	39.1%	63.3%	48.7%
Chemotherapy	0	31.3%	46.8%	34.8%
Radiation	0	13.7%	18.8%	14.6%
Diabetes	0	11.7%	12.5%	11.2%
Smoking	0	19.6%	12.5%	15.7%

Table 2.1. Unprecedented control of variation leads to better comparisons. Utilizing capsule tissue from temporary expanders effectively removes the variable of implant residing time. Additionally, a single implant type further removes variables proven in previous literature. This method provides cleaner comparisons of other variables.

Variable Selection

Copious risk factors have been explored for correlation with capsular contracture. Variables were selected by identifying commonalities in previous studies, as well as screening for ease of collection (e.g., not requiring additional diagnostics or additional data collection by the physician). To this end the following were used:

Patient age (years)
Chemotherapy (yes or no)
Radiation (yes or no)
Diabetes (yes or no)
Smoking (yes or no)

When two-stage reconstruction is used, the capsule formed can be used for additional predictive metrics. Histological variables were collected on a subset of patients to evaluate the importance of further diagnostics and enhanced monitoring of capsule severity. Capsule tissue thickness and vessel size were selected because they could be measured by non-invasive procedures, such as MRI or ultrasound, given sufficient justification for the additional cost. Implant residing time was also considered.

Model Training and Validation

Ordinal Logistic Regression: With the lack of a continuous clinical scale of severity, the clinical Baker scale of capsule severity was used as ordered categorical dependent variable. Independent variables were categorical (e.g. radiation, chemotherapy) or continuous (e.g., patient age, residing time). Model components explaining less than 5% of variability were discarded to simplify the model.

Bootstrap Forest Model: This type of model generates a large number of decision trees. Individual decision trees suffer from overfitting the training dataset so by generating a random forest trained on different parts of the same data set reduces the variance and improves performance. This type

of partitioning describes the relationship between a response and a set of variables that may influence it. Each tree divides the data into groups which are maximally different with respect to grade. The output of a forest is the mean prediction of the individual trees. Variables can be ranked by their ability to predict variation in grade.

Artificial Neural networks: Models were developed in SAS JMP software. The models' initial seed was specified to allow comparability between models. The data set was split into 5 subgroups, 4 were used for training and the fifth was used for validation via the k-fold method. Various node and layer combinations were tested. The optimized model was constructed with 2 hidden layers each with 1 hyperbolic tangent node and one linear node. Each model was given a boost of 10 with a learning rate of 0.1 generating 20 total nodes per layer and allowed 25 rounds of refinement. The model was free to transform covariates with a squared penalty.

2.4 RESULTS AND DISCUSSION

Histological Evaluation

Capsule tissue derived from silicone shell expanders has been demonstrated to closely mimic the structure found in capsules from silicone gel implants. [32,36,130–133] and this proved true in our hands as well (Figure 2.1). The differences between capsules is largely due to differences in residing time, e.g., vascularity and cell density decrease over time. Residing time matched capsules from both implant types are grossly indistinguishable. A notable difference seen in this histological analysis was the relative relaxation of collagen matrix in young expander capsules (Figure 2.1, E), while implant capsules that have been in place several years, show a linear collagen structure presumably from completed crosslinking of the structure. Like capsules from permanent implants, expander capsules have a defined interface region (Figure 2.1, G) that is marked by increased cell density. [33,131,134,135] Thus, capsules formed around silicone shell expanders serve as an excellent model for early capsule development around more permanent silicone implants, allowing variable control not possible in other human experimental designs.

To further explore this experimental model, numerous clinical and histological aspects were evaluated and analyzed for correlation to grade as well as to each other. Capsule thickness did not correlate to capsule grade, however, interface thickness was significantly smaller in Grade I capsules (Figure 2.1, B & C). Additionally, vessel size increased while density decreased with capsule grade ($P<0.05$, Figure 2.1,D).

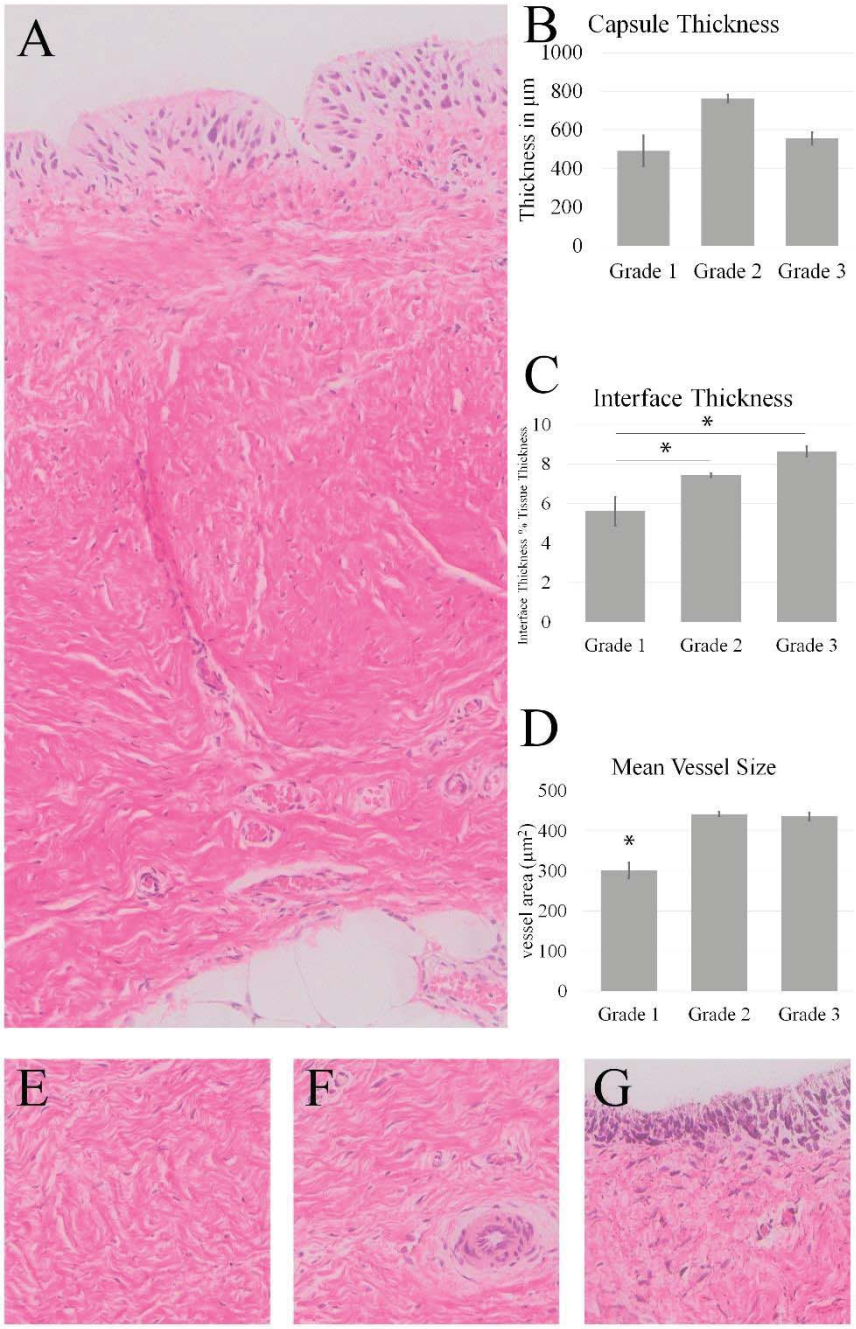

Figure 2.1. Gross histology of expander-derived capsules is similar to those from permanent implants. A) Capsule tissues are characterized by an implant interface (G), a collagen dense middle region (E) and a more vascular region at the tissue interface (F). Interface thickness was found to be significantly smaller in grade 1 capsules (C), while tissue thickness showed no difference across capsule grades (B). Finally, vessel size is increased in higher grade capsules (D). *P<0.05

	Smoking	Diabetes	Radiation	Chemotherapy	Residing Time	Patient Age	Cancer	Vessel Size
Tissue Thickness	0.627	0.113	*0.075*	0.829	0.530	***0.026****	0.640	0.210
Vessel Size	0.652	0.658	*0.096*	0.776	0.353	0.722	0.933	
Cancer	0.381	0.713	***0.003****	0.155	0.938	***0.028****		
Patient Age	0.360	0.611	0.916	*0.065*	0.172			
Residing Time	0.535	0.294	0.277	0.981				
Chemotherapy	0.762	0.308	*0.054*					
Radiation	0.999	***0.035****						
Diabetes	***0.008****							

Table 2.2. Clinical variables were found to correlate to each other. The table presents p-values of correlation between each variable pair. *P<0.05

Variable Exploration

Logistic fit showed that no single variable correlated to capsule grade and that variable crosses were largely irrelevant. The variable relationships, observed in this correlation matrix Table 2.2, suggest the population being studied generally show relationships reported previously.[136–138] For this data set, patients with diabetes were more likely to be smokers. It remains to be determined whether this observation would hold in larger populations or other regions, but may reflect a lifestyle evident within our cohort. Intriguingly, patients with diabetes were also more likely to receive radiation therapy, though the basis of this link is unclear.[139] The data also demonstrate a correlation between patient age and cancer risk, which is well documented.[140,141] The final observation is that older patients produce thinner capsules, possibly related to mechanisms that result in generally poor wound repair responses in older individuals. [142]

Because ordinal logistic regression failed to predict meaningful influences on capsule grade, additional methods were explored. SAS JMP's predictor screening was used to evaluate the predictive power of each variable. This software uses a bootstrap forest model, and the variable contributions to the prediction of capsule grade are ranked[143] The model was run 10 times to mitigate the stochastic nature of forest models.

By this method, patient age, chemotherapy, mean vessel size and tissue thickness emerged as the greatest predictors of capsule grade (Table 2.3). Interestingly, smoking [144], radiation and diabetes, commonly cited risk factors [142], all contribute to less than 5% to grade prediction. The basis of this discrepancy is not clear. It may suggest that such factors have greater impact over longer periods of implant residing time, as has been typical in other clinical assessments of capsular contraction, which may involve capsules formed over many years. As shown in Table 1 the average residing time of the capsules assessed here is 3-4 months. It also noteworthy that temporary expanders produce a higher strain environment, and this may elicit sensitivity to variables that differ from those associated with the more static permanent implant environment.

	Mean %	STD	COV
Patient Age	23.9	5.12	0.21
Chemotherapy	18.1	3.71	0.20
Mean Vessel Size	15.8	5.19	0.32
Tissue Thickness	13.9	3.25	0.23
Residing Time	8.5	2.84	0.33
Cancer Side	11.7	3.43	0.29
Smoking	4.5	2.11	0.46
Radiation	2.3	1.16	0.50
Diabetes	1.0	0.57	0.57

Table 2.3. A Forest predicts the most important factors in determining capsule severity. Ten forests were generated and the percent of variation explained was averaged across all models to accommodate the stochastic nature of decision trees. The mean percent of variation explained is presented along with the standard deviation and a coefficient of variance. This model predicts patient age and chemotherapy treatment are the most important determinants of capsule grade.

Artificial Neural Network

Logistic regression also suggested that variables were not interacting to influence capsule grade; however, variables are correlated to each other (Table 2.2) and intuitively should be impacting each other. Artificial neural networks have been successfully used for diagnostic prediction of conditions with complex inputs.[128,129,145] Within a network, inputs are selected and allowed to interact within layers at numerous nodes, largely free of preconceptions. The model is then run to optimize coefficients at each node to determine the weight of the information entering the node.

To begin the number or layers and form of node interactions need to be optimized by trial and error. Various configurations of layers and nodes were tested with a sample of inputs. This resulted in the selection of a two layer model with both hyperbolic tangent and linear nodes. Based on the magnitude of the coefficients, the model puts more weight on the hyperbolic tangent nodes but the linear portion of the model is not insignificant.

Numerous networks were then developed using varying configurations of input variables. Increasing the number of inputs improved the overall model fit and reduced the misclassification rate. This work suggests that cancer side is redundant and added little to the model performance. For the patient population studied, the presence of cancer and radiation treatment were strongly correlated ($P<0.01$). This is not a surprising finding, but it is an association which may not be as influential in a larger data set, thus it was kept in the final model.

Purely clinical variable inputs were only able to account for approximately 70% of variation (Figure 2.2a). Adding capsule thickness and/or vessel size considerably improved model performance (Figure 2.2b), together accounting for nearly 30% of variation. Including both variables also improved the misclassification rate to 4.5%. Implant residing time further improved the model; yet, when considered in larger context, residing time would ideally be the remaining lifespan of the patient. The input data here is ill-equipped to predict outcomes for long term implant life span.

A

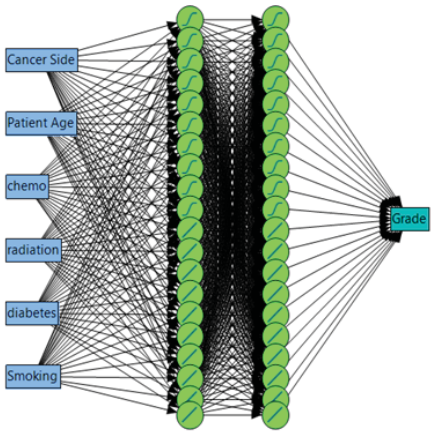

a

	Training	Validation
Generalized R^2	0.62	0.67
Misclassification Rate	28%	18%
ROC	.92	0.98

B

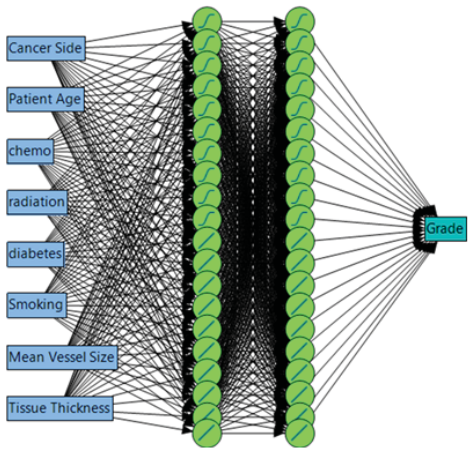

b

	Training	Validation
Generalized R^2	0.91	0.94
Misclassification Rate	4.5%	0%
ROC	.997	1

Figure 2.2. Including vessel size and tissue thickness drastically improves model performance. While the receiver operating curve areas are good in both cases, the smaller model lacks fit and predictive power.

With this in mind the model represented in Figure 2.2B was selected for further investigation. The model was run many times to optimize the performance. The final model produced and R^2 between 0.91 and 0.94 and had a misclassification rate of 4.5%. Interestingly, the overall weighting of inputs largely aligned with the forest model, with patient age being the most weighted variable. JMP's profiler tool was then used to evaluate clinical scenarios with the model.

A patient age 50 with unilateral cancer who receives chemotherapy but has no other risk factors, has a very high risk of asymmetry. Setting the tissue thickness and vessel size equal, the non-cancer side has a 95% chance of developing a Grade II contracture while the cancer side has 98% chance of developing a Grade III. Interestingly by increasing mean vessel size beyond 26μm in diameter can drastically reduce the risk of Grade III in the cancer side to 6%. While it is unclear how vessel diameter will correlate to clinical proxies, this may suggest that local vasodilators or increasing vascularity could be used to address asymmetry.

In more generalized cases, the model also predicts a strong influence of vessel size, a proxy for blood flow, on risk of Grade III contracture, particularly in cases with radiation treatment. Radiation is known to impact wound healing via various mechanisms[137] including vessel formation.[146] We have found that vessel size is reduced in capsules subjected to radiation treatment (data not shown).

This model suggests the potential benefit of modulating blood flow during capsule formation to improve capsular contracture outcome when radiation is required. Interventions could include treatment with growth factors such as VEGF or small molecule vasodilators. Conversely, other work has shown that the presence of blood in the implant pocket is correlated to increased capsule grade. [147] Because of this patients are asked to stop any blood thinning drugs 10 days prior to surgery. Recent work by Chuba et al demonstrated that depressed patients had an increased risk of severe capsular contracture. These patients are generally not asked to discontinue treatment for obvious reasons; however, common treatments include SSRIs which are on par with NSAIDs for their activity in blood thinning. It is possible the blood thinning treatment is what links depression to capsular contracture. [148] Further work is needed to clarify the direct influence of blood flow on capsule severity and to identify key temporal intervention points.

If the same patient is also a smoker, they can reduce their risk of Grade III contracture further by becoming a non-smoker. Granted a non-smoker is not equivalent to a past smoker, but further work with an increased training set could better delineate subtypes within variables that are currently binary. This result is particularly interesting in light of the fact that the logistic regression analysis did not indicate a large effect on capsular contracture severity. Diabetes is another such factor which could be expanded to account for blood sugar levels. The ANN model evidently identifies smoking can be a key determining factor for a given patient, depending on the context of other factors smoking finds itself associated with. Diabetes is another such factor which could be expanded to account for blood sugar levels. With further improvement, this model could be transformed into a preprogrammed calculator to help doctors advise their patients of their individual risks and help advocate for lifestyle choices that could improve reconstructive outcomes.

Strengths and weaknesses of the Study

There are limitations to our study. The first is the use of a subjective clinical scale for a disease that has a continuum of outcomes. This method is standard within the field and is in many ways the most practical way to classify capsules given a lack of other definitive measurements that directly correlate to capsule severity. Some efforts [130,149] to provide a more objective scale have been attempted but are largely irrelevant to the clinician, who is not likely to perform detailed histology or invasive measurements when that additional information doesn't assist in making practical decisions on the welfare of the patient. Further understanding of mechanism, as well as use of imaging technologies, may eventually provide more objective approaches to the measurement of the clinical severity of capsular contracture.

A major design criteria for this model was that input variables be easy to access for a clinician; however to obtain optimal predictive power, capsule thickness and a proxy for blood flow were required. While ultrasounds are relatively common for breast cancer patients, Doppler flow ultrasound is not. Given the large improvement these variables provide it is worth further study and cost analysis to determine the viability of performing Doppler flow ultrasound on patients

undergoing breast reconstruction. Alternatively, some handheld devices have been developed blood flow or proxies which could be evaluated as lower cost options. For example, Butterfly iQ is a handheld ultrasound that plugs into smart phones[150] and might be worth further evaluation as a practical solution for clinicians making evaluations and decisions on patients who are undergoing breast reconstructive surgeries.

Future work on this model will require the expansion of the training. The 89 patient cohort described here loosely matched the CDC numbers for smoking[151] and diabetes[152] and shows similar occurrence rates for each capsule grade to larger studies.[153] That said, the absolute number of patients with each complicating factor are relatively small.[20,21] With a larger cohort finer detail could be built into the model, such as type I and type II diabetes or non-smoker, current smoker and past smoker.

Implications for clinical practice, patient education and research

The risk of poor outcomes from plastic surgery are often not understood by patients. Using this model as a streamlined calculator in a clinic setting can visually demonstrate risk to the patient and help them to make more informed decisions about their treatment. Additionally, physicians can use the tool to demonstrate the impact of lifestyle choices such as smoking on the patient's reconstruction outcome. Having a hard number of risk resulting from the combinatorial effects of lifestyle choices could improve patient compliance with physician recommendations.

Furthermore, the model predicts a number of potential interventions which could mitigate capsule severity and asymmetry. Additionally, it predicts which subset of patients are likely to benefit from such a treatment so that the intervention can be targeted for each individual. Each of these treatment predictions need further validation both at a basic science level and in clinical settings.

Conclusions

The ANN model presented here is a novel approach for predicting capsular contracture severity in a patient specific manner. The neural network approach allows a greater degree of interaction between inputs and has generated a model that can potentially be used as an interactive tool to optimize risk assessment for each patient in a personalized manner. Furthermore, the model has suggested modulation vascularity could be an important intervention when radiation treatment is indicated.

CHAPTER 3: Characterization of scar capsules around temporary expanders in breast cancer patients undergoing reconstructive surgery: a novel model for probing mechanisms of capsular contracture

3.1 ABSTRACT

In capsular contracture, a robust scar surrounds the implant begins to contract, distorting implant shape and at times causing pain. Clinically, this contracture is graded from I to IV on the Baker scale, with III and IV being the most severe grades. While extensively studied, the largest difficulty still facing the field is extreme variation in study design. Here we describe a standardized human model of capsular contracture which makes use of silicone shell temporary expanders. By using capsules formed around expanders, there is greater uniformity in implant type and residing time. This model has been combined with detailed quantification of the capsule tissue generating new insights about capsular contracture development. Capsule vasculature decreases in density ($P=0.06$), while increasing in cross-sectional area ($P<0.05$) as capsule severity increases. Because the residing times are equal between groups, this suggests that the vascular beds of more severe capsules are maturing more quickly or completely. The matrix was then assessed with Picrosirius red staining under polarized light, where red birefringence is related to fiber size or maturity. Grade I capsules have less red birefringence than either Grade II or III ($P<0.01$). Collagen IV localized to the implant interface, overlapping with the highest densities of CD68+/CD163+ macrophages. Just beyond this region, activated fibroblasts (αSMA+/Vimentin+) are at their highest density. The interface of these two cell populations could be a key nexus informing capsule structure.

3.2 INTRODUCTION

The five year survival rate for breast cancer is approaching 90% [154] and women are able to think about life beyond cancer. Between 2000 and 2016 there was a 39% increase in breast reconstructions, 80% of which were implant based. [3,9,10] The most common cause of revision in these patients is capsular contracture, a foreign body reaction that has a reported incidence between 3 and 50%. [7,12,15–17] In capsular contracture the scar tissue surrounding the implant begins to contract and distort the implant shape and in some instances cause pain. Clinically, this contracture is graded from I to IV on the Baker scale, with III and IV being the most severe grades. [124]

Current knowledge of capsular contracture is largely based on capsule tissue derived from permanent silicone implants. Capsule tissue is a specialized type of internal scar tissue, which is largely composed of fibrous matrix and contractile fibroblasts and some residual inflammatory cells.[34,37,132] Traditional models of fibrosis indicate that the immune system, macrophages and upstream interactions with T cells, regulate the phenotype of fibroblasts. The contractile nature of the capsule is largely attributed to myofibroblasts and the acellular matrix of capsule [30,155]. Yet, it is becoming increasingly evident that the signaling driving the formation of fibrotic tissue is a two-way street, involving back and forth interplay between the different cell types comprising the scar and the matrix.[55,156,157]

Research into the mechanistic basis of capsular contracture has been limited by the lack of suitable and standardized models to study this phenomenon. Animal models can provide general insights into the foreign body response driving fibrous envelopment of implanted materials. Nevertheless, animals do not recapitulate the full-blown pathology of capsular contracture observed in humans. Research on capsular contracture in patients has also presented challenges, driven largely by the understandable and necessary limitations on such studies. For example, samples are typically derived from patients who have elected to have revision. This likely causes unavoidable biases in the tissues collected, including that samples are generally limited to the more severe cases. Conversely, capsules of the lowest severity (Grade I) are infrequently collected, constraining the range over which are comparisons can be made. Perhaps most significantly, many past studies have reported results from scar tissue derived from revisions that may take place anywhere

between 6 months to 20 or more years after the initial surgery – confounding the identification of factors contributing to severity of capsular contracture.

In this study, we attempt to address limitations of prior work by utilizing residing-time standardized capsule tissues from temporary expander implants derived from the two-stage reconstruction procedure. Collecting capsules at a consistent anatomical location from these silicone shell expanders at around 4 months following implantation allows for smaller temporal variation than previous studies, while maintaining clinical relevance for cancer patients. The use of this model may enable improved evaluation of histological, biochemical and genetic factors that contribute to capsular contracture in breast reconstruction, as well as providing insights into the peri-implant fibrotic process for the range of devices, including other soft implants, pacemakers and artificial joints, that are implanted in the human body.

3.3 MATERIALS AND METHODS

Sample collection

All patients had textured silicone shell saline filled tissue expanders and samples were collected at the time of expander removal. Patients with connective tissue disease or other diseases associated with abnormal wound healing were excluded. Patients with a history of keloid or hypertrophic scarring were not excluded however less than 1% of this population fits this description. The plastic surgeon (Dr. Moyer) collected a rectangular capsule sample from the 12 o'clock position of the implant under IRB Protocol #1289. Tissues were fixed within 3 hours of excision in 4% paraformaldehyde for 24 hours then washed and stored in ethanol until paraffin embedding. Clinical variables were stored in a de-identified database.

Picro Sirius Red staining

Paraffin embedded tissues were cut into 5μm sections. Tissues were dewaxed in xylene and ethanol then incubated 1 hour in Picrosirius Red (PS) stain. Slides were then washed twice in a dilute HCl solution, dehydrated in a series of ethanol and xylene washes. They were imaged at 20x using an Olympus VS120 slide scanning microscope set for polarized light microscopy to generate large high resolution images of the full tissue.

Custom matlab code was created for analysis. *R/G Ratio:* RGB format tif images were converted to HSV format and hue ranges were parsed into red and green. Tissues were masked to exclude vascular voids and regions of empty slide. For the remaining tissue total number of red pixels and total green pixels were combined to create a ratio to indicate the relative proportion of mature to immature collagen in each tissue. Analysis was optimized on a subset of images and then converted to a batch process. *Entropy:* Additionally, code was designed to evaluate the disorder of the tissue. RGB tif images were converted to greyscale and the Shannon entropy was calculated for the tissue. The value was then converted to 1-entropy for easier interpretation.

Tiling

In an effort to improve accuracy of calculations within the heterogeneous tissue, the high resolution images were subdivided into tiles. The rationale for this was to give more weight to local region values that may be overwhelmed in a whole image analysis. Tile sizes ranged from dimensions of 11 μm^2 to 56 μm^2. The best discrimination between capsule grades occurred at 33μm^2. For each tile, a green to red ratio was calculated. Then the tile values were averaged to consolidate data into a single value per tissue section, in order to prevent misleading results from inflation of the sample numbers.

IF Staining

Paraffin embedded tissues were cut into 5µm sections and underwent antigen retrieval (EDTA pH 8, for 3 min in a pressure cooker). Tissues were blocked with 1% BSA and incubated overnight at 4°C in primary antibody. Alexa flour secondary antibodies were incubated 1 hour at room temperature. Hoescht nuclear stain was applied in the second of 4 washes prior to mounting with Prolong Gold.

Integrated density: for selected tissue areas was calculated using ImageJ.
Myofibroblasts: tissues were stained for αSMA and vimentin. A mask was applied to remove vessels positive for αSMA. Only nuclei with corresponding αSMA and Vimentin staining were considered myofibroblasts. The cell count was normalized for area to create cell density. *Macrophages:* tissues were stained for total macrophage marker, CD68 and either the M2 marker CD163 or the M1 marker CD86. The total number of CD68+ cells were counted. Only nuclei with corresponding CD68 and secondary marker staining were considered polarized macrophages. The cell count was normalized for area to create cell density. *Depth distributions:* Custom code was generated to semi-automatically identify the implant interface, the tissue surface in contact with the implant when in vivo, in each image. Than interface was represented as a single line in a mask which could then be dilated to a given depth. Tissues were analyzed, for cell count or staining density in 300 pixel strips from the implant interface.

3.4 RESULTS

	Grade I	*Grade II*	*Grade III*	*Total*
n	***4***	***24***	***22***	***50***
Patient Age	***57.7 ± 3.5***	***45.3±9.6***	***51.2±13.13***	***48.9±11.5***
Residing Time	***3.75±1.5***	***3.83±1.6***	***3.9±1.0***	***3.86±1.3***
Chemotherapy	***0***	***37%***	***45%***	***38%***
Radiation	***0***	***8%***	***22%***	***14%***
Diabetes	***0***	***0***	***9%***	***4%***
Smoking	***0***	***8%***	***9%***	***8%***

Table 3.1 Utilizing capsules formed around expanders allows residing time to be very consistent and removes implant type as a variable

Cohort description

The cohort of capsules described here contained 50 capsules with severity scores ranging from Baker score 1 to 3 with an average residing time of 3.86 months (+/- 1.3). All patients were undergoing immediate bilateral two stage implant based reconstruction post-mastectomy. These capsules were selected from the larger population described in chapter 2. More in depth staining was too cost prohibitive to include all patients. Tissues that could not undergo antigen retrieval protocols had to be excluded. This work standardized tissue processing to provide the most comparable results thus the tissue preparation was not optimal for all tissues and some tissues could not be analyzed. No Grade IV capsules were collected during this study, as the key differentiator between Grade III and IV capsules is the presence of pain. Pain develops when the capsule entraps a nerve, a relatively stochastic event with no known connection to contraction of the capsule.

Matrix structure

Capsule tissues were stained with PS in order and then imaged at high resolution across the whole tissue to evaluate capsule structure (Figure 3.1 a). In addition to structural detail, PS viewed under polarized light provides a spectrum of birefringence which is thought to correlate to fiber maturity, though probably more strictly relates to fiber thickness. [158–160] With this imaging technique, previous work has shown that higher grade capsule tissue have more red fibers than lower grade capsules.[31] This result was confirmed with our patient cohort; however, the difference was small. Detailed inspection of the high resolution montages of tissue sections consistently revealed sub regions or "blobs" of mature collagen within the tissue that showed more red birefringence than surrounding tissues (Figure 3.1a, arrows). This phenomenon may have been observed as the capsular samples under study here were derived earlier time point than previous studies. We deduced that the size and variance of this interesting heterogeneity in collagen structure might be lost over the large scales that we assessed implant structure – putting this another way, a global green/red ratio would effectively average out these regions of greater maturity, simultaneously increasing unexplained levels of variance within the measurement (Figure 1b).

To evaluate the impact of these 'collagen blobs' within the scar tissue, images were divided into a range of tile sizes to determine the best 'resolution' for observing these units (Figure 1c). Once the optimal tile size was selected, the images were evaluated for each tile and then averaged to generate a single value per tissue. This approach allowed extreme values to be more represented in the tissue average and provide better discrimination between capsule grades, without artificially improving significance with inflated sample numbers. With this tiling method a number of variables were evaluated including staining density, fiber orientation, green density, red density, ratio of green to red and entropy. Only the ratio of green to red and tissue entropy were significant, suggesting that when substructures were accounted for, Grade I capsules have thinner matrix fibers and more disorder in their structure than higher grade capsules (Figure 1d,e). By tiling the images, the subunits could be further analyzed by plotting the number of green and red tiles over a range of tiles sizes. This produced an intersection point which suggests a characteristic tile size at which red birefringence begins to dominate the tile, a proxy for subunit (i.e., blob) size. Grade III capsules have a larger tile size of intersection suggesting larger units of red birefringent collagen or larger subunits within these tissues.

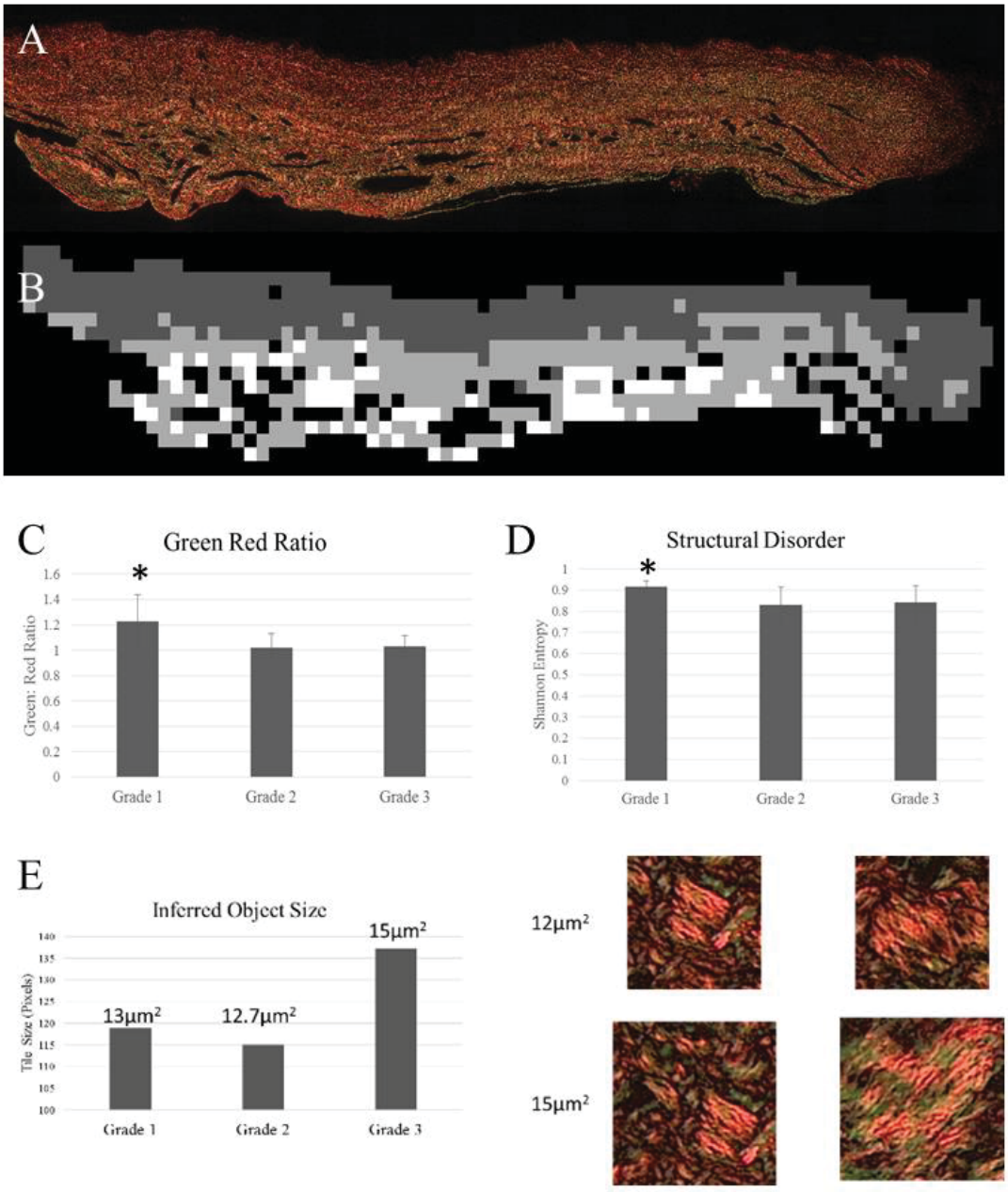

Figure 3.1 Picrosirius Red staining identifies novel subunits within the young capsules A) PS staining, viewed under polarized light, enhances the natural birefringence of collagen fibers. Red birefringence is associated with larger of more mature fibers while green is associated with thinner less mature fibers. B) Map of local red green analysis at 200x200 pixels. The values have been binned into three levels and remapped on to the image. C&D) With this method of analysis, it is possible to discern differences in red:green ration and disorder of the tissues. E) By evaluating at what tiles size red began to dominate the image, an inferred mature collagen object size can be calculated. A small object would be averaged out in larger tiles.

Collagen Expression

A limitation of PS staining is its broad staining of all collagens. In order to evaluate which collagens were related to the differences seen in fiber thickness and disorder, key collagens were analyzed. This isoform specific staining of collagens showed no evidence of the substructures observed with PS, suggesting that these regions are a result of orientation or crosslinking rather than a shift in collagen type.

Traditionally, collagens I and III are considered markers of the fibrotic process (i.e., more collagen III compared to collagen I is considered less pathologic).[161] Collagen VI, while less commonly associated with wound healing, has been shown to have significant impacts of matrix structure.[162] The total quantity of collagen I and III, as assessed by integrated density, did not vary between capsule grades. The ratio between the two collagens was also not changed with grade. The subunit structures seen in PS stained tissues were not visible by immunofluorescence for the collagen subtypes stained. This suggests these subunits are defined more by fiber alignment/angle than by a particular collagen profile. Interestingly, collagen VI was more highly expressed in Grades II and III compared to Grade I (Figure, 3.2, D, $p<0.05$). In addition, collagen VI was found to have an increased density at the implant interface compared to the rest of the capsule thickness (Figure 3.2 C, E). This bias in distribution was not observed in the other collagens.

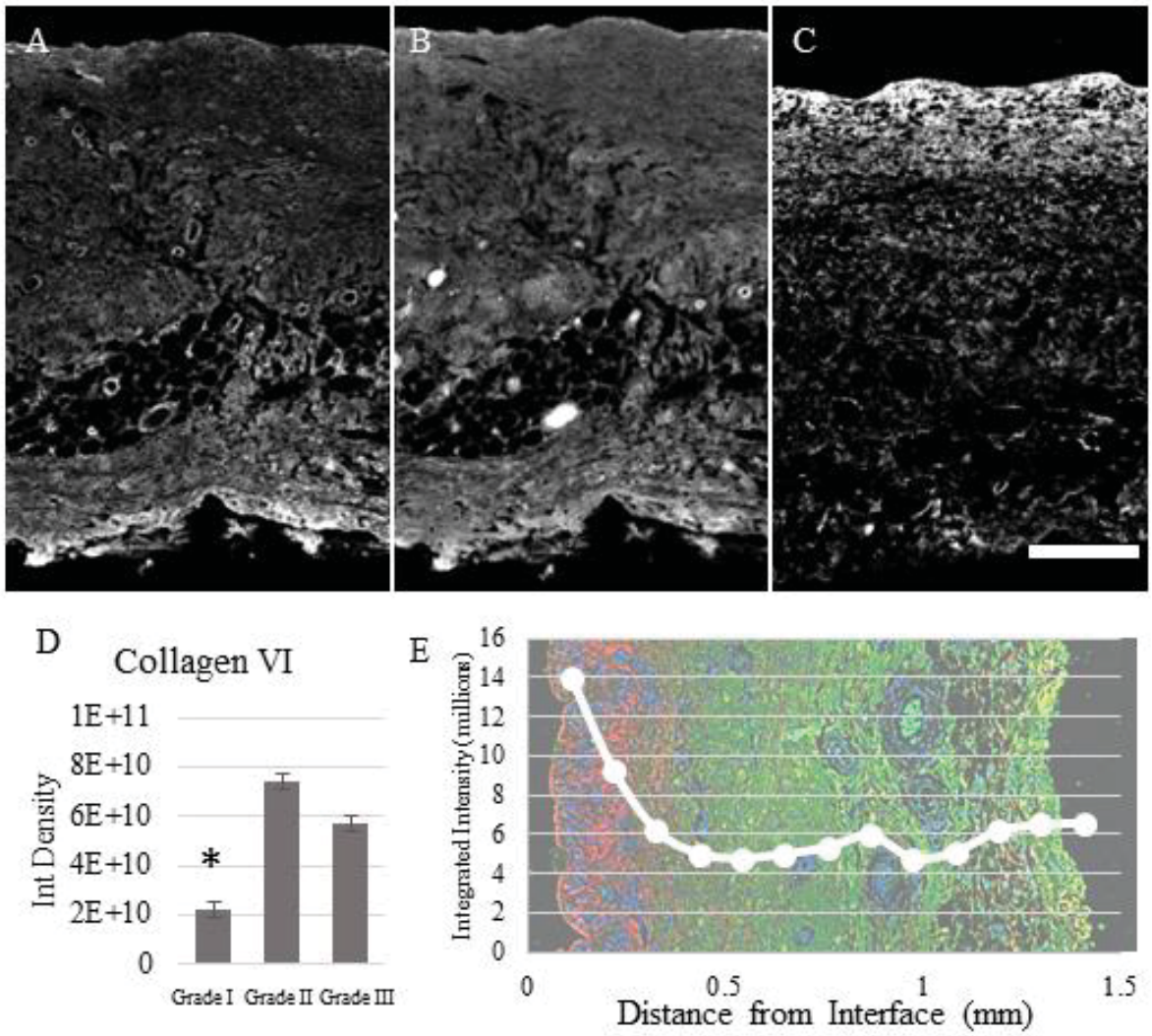

Figure 3.2 Collagen VI emerges as a key collagen of interest both in quantity and distribution A) Collagen I B) Collagen III C) Collagen VI. D) Overall quantity of collagen VI was significantly lower in grade one capsules. E) Across all grades, collagen VI was preferentially located at the implant interface.

Fibroblast Activation

The final matrix construction is an output of a highly dynamic wound healing response involving various cell types. The most direct influence on matrix structure comes from fibroblasts. Tissue was stained for vimentin and smooth muscle alpha actin to identify activated fibroblasts, commonly implicated in excess fibrosis (Figure 3.3a). To ensure rigor in our analyses, only cells with stained nuclei that were also positive for both vimentin and αSMA were considered to be activated fibroblasts (Figure 3.3b, arrows). Total cell density was not different between capsule grades. Fewer activated fibroblasts were found in Grade I capsules ($p<0.01$, Figure 3.3c). Across all capsule grades, activated fibroblasts had the highest density between ~100 and 200μm from the implant interface (Figure 3.3D). The matricellular protein CCN1 has a key role in regulating fibroblast activation[163] and was identified in our RNA-seq is significantly associated with capsule grade (Figure 5.3). Myofibroblasts excrete large quantities of CCN1, which can act as a mechanism that slow activation of fibroblast populations by triggering quiescence and apoptosis.[164] Typically, as more myofibroblasts differentiate in a wound and begin producing CCN1 the healing process is resolved[163,165], thus a less pathologic capsule might have more CCN1 shutting down fibrosis more quickly. Paradoxically we determined that CCN1 was increased in Grade III capsules compared to those of Grade I and II (Figure 3.3 F). Interestingly, CCN1 levels were lower in capsules that had been irradiated compared to those that were not.

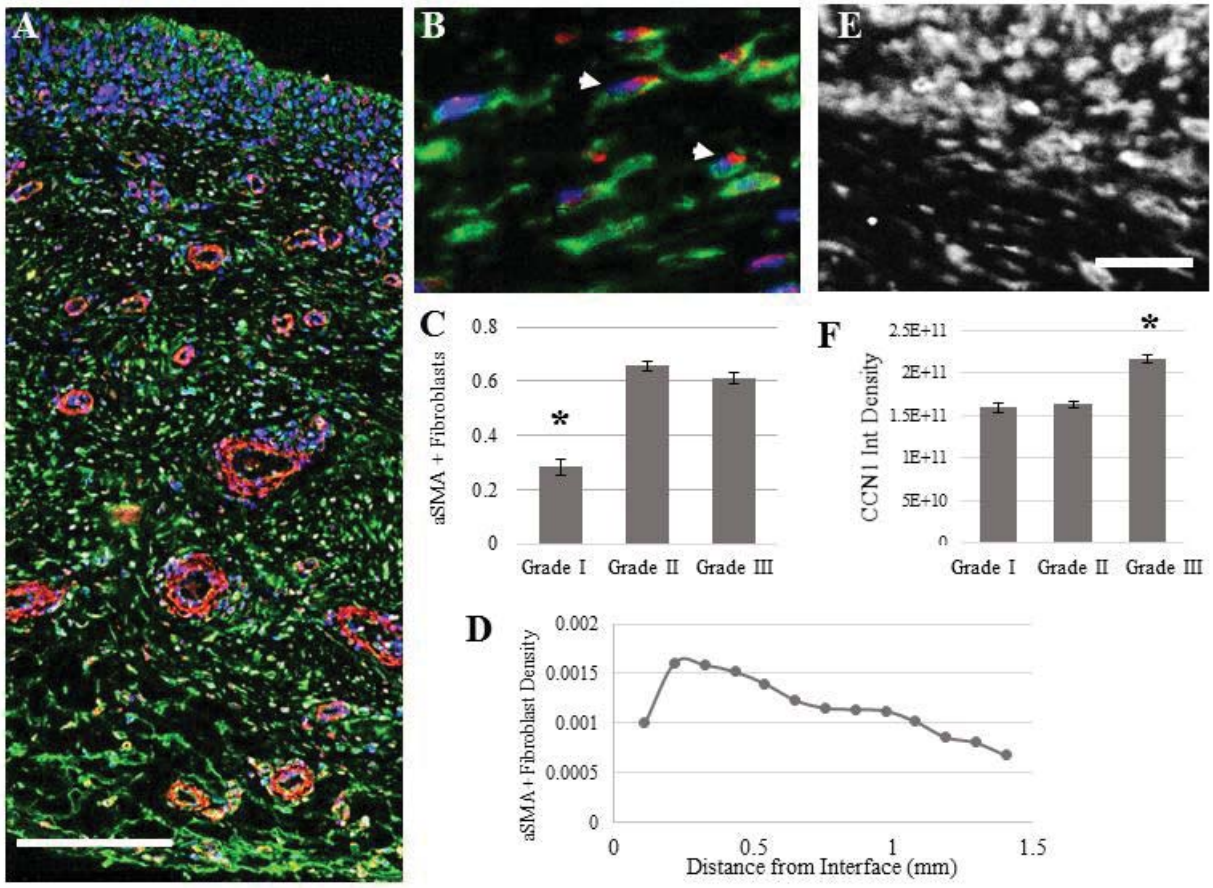

Figure 3.3 Fibroblast activation is increased in higher capsule grades A) Nuclear (blue) aSMA (red) and Vimentin (green) stained capsule tissue with the implant interface located at the top of the image. aSMA+ Vessels were removed for fibroblast analyses. B) Arrows denote examples of countable myofibroblasts results of the quantification are found in C and D. E) CCN1 staining observed near the implant interface, integrated density is quantified in F. * $P<0.05$ Scale for A is 100µm, Scale for B and E is 50µm.

Macrophage Phenotype

Macrophages can be generally grouped by phenotype into classically (M1) and alternatively activated (M2). M2 macrophages have additional sub classifications but are generally associated with improved implant tolerance and wound resolution[166,167]. Capsule tissue was stained for CD68 a total macrophage marker, CD86 an M1 marker, and CD163 an M2 marker to obtain a general overview of macrophage phenotypes. Total and M1 macrophages did not vary with capsule grade. M2 macrophage density was highest in Grade I capsules and was indirectly correlated to capsule grade (Figure 3b). When evaluating distribution, increased capsule grade correlated to a higher density of macrophages at the implant interface (Figure 3c). Further subdivision by phenotype showed that M2 macrophages were more closely associated with the implant interface in lower grade capsules (Figure 3 d), while M1s had a uniform tissue distribution. Foreign body giant cells were not observed in capsules in this study, possibly attributable to the fact that only capsules of less than 3-4 months residing time were under investigation.

With further investigation into cell and matrix distributions across tissue depth, an interesting organizational pattern emerged. M2 macrophages appear to make up the majority of cells at the implant interface and are known to produce collagen VI which also localizes to the implant interface. Myofibroblasts are at peak density just below the M2/Collagen VI region. Collagen VI did not correlate to tissue thickness or the red green ratio in our cohort of patient tissues.

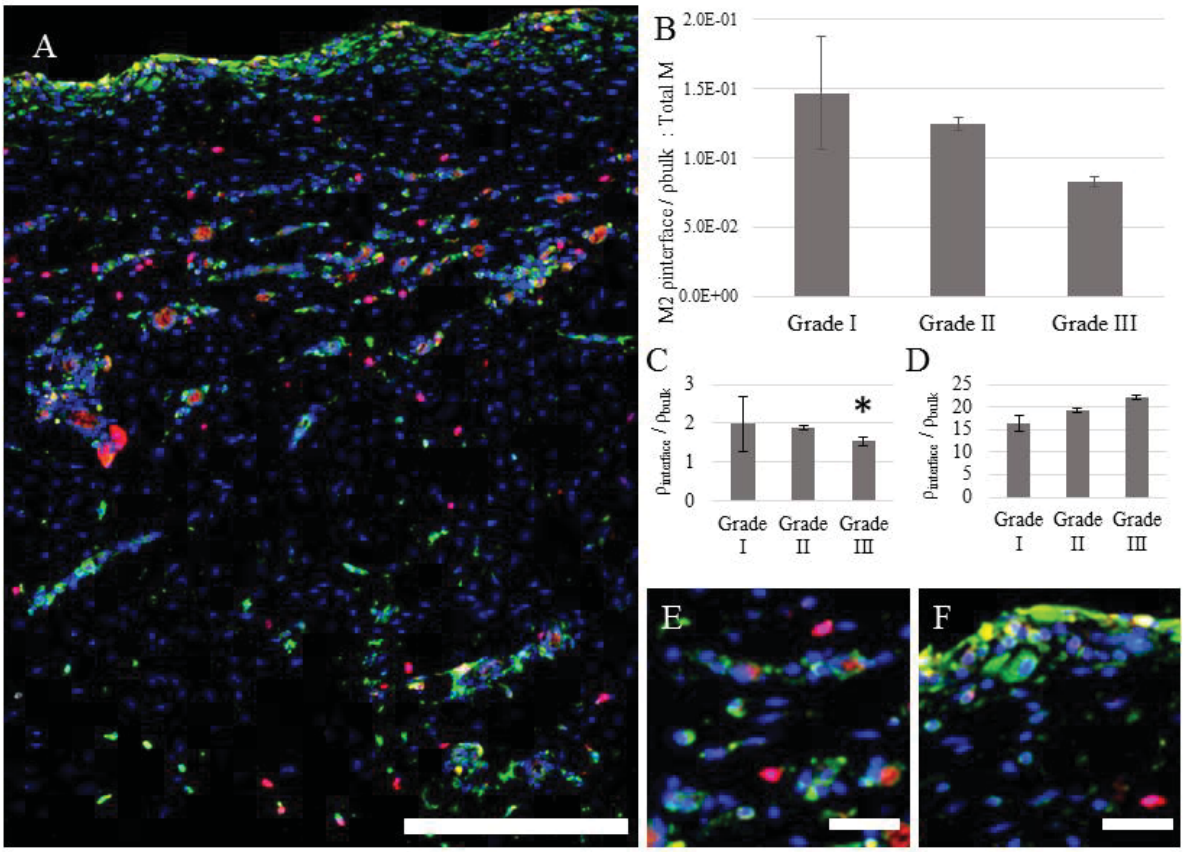

Figure 3.4 M2 Macrophages are more closely associated with the implant interface in lower grade capsules Capsule tissue stained for nuclei (blue), CD163 (green) and CD68 (red). Nuclei associated with CD68 staining were considered macrophages while nuclei positive for CD163 and CD68 were considered M2. C) The ratio between M2 density at the interface and the bulk of the tissue demonstrates that grade III capsules have significantly less bias towards the interface. D) The opposite trend is seen for total macrophages. B) represents the combination of these two trends. *P<0.05 Scale A 100µm, Scale E and F 50µm.

3.5 DISCUSSION

The foreign body response, and by extension capsular contracture, is a dynamic inflammatory process.[37] By employing capsule tissue from temporary expanders, tissue can be sampled and compared at a uniform time point (3-4 months post-implantation surgery) can be evaluated and thus comparisons between fibrotic markers in different capsule grades can be undertaken in a more precise manner. This work has been able to meaningfully evaluate variables across capsule grade and find correlations that were previously obscured by high degrees of capsule to capsule variation that characterize most previous studies.

Novel analysis of PS stained capsule tissue identified small sub-regions of increased red birefringence which have not been described previously. It's possible these regions are reminiscent of crystal nucleation sites, in that they may be regions of a particular order which propagate outward until meeting another unit Nucleation is defined as the formation of either a new thermodynamic phase or a new structure via self-assemble which generally occurs at impurities. In the context of capsule formation, a nucleation site could be considered a point where a certain signaling molecule has concentrated or a sub population of fibroblasts has become stimulated in a certain way. Understanding this development process could inform future interventions.

The present study finds that myofibroblasts are present at higher densities in higher grade capsules compared to those of Grade I, while overall cell density and vimentin positive cell density are unchanged. In contrast, Hwang et al. mechanically tested capsule tissue and determined that myofibroblast density, as discerned by αSMA trended with but was not correlated to contractility, which was correlated to grade suggesting a disconnect between activated fibroblasts and contractility.[30] It is possible the more rigorously standardized model used here allowed greater discernment in trends that were previously obscured by variability. Another possibility suggested from the literature is that while smooth muscle actin is a common marker of fibroblast activation, fibroblasts without this protein may still contribute to contraction.[72] Other work has suggested metabolic changes are required for fibroblast contractility.[168] The discontinuity between the results shown here and previous literature could be due to an incomplete picture of the contractile cells in the capsule. It remains unclear the exact contribution of capsule fibroblasts to contraction. Kyle et al have demonstrated that capsule fibroblast can maintain phenotype in culture and conditioned

media from these cells is sufficient to increase collagen gel contraction of normal fibroblasts.[169] More work is needed to assess this type of activation. It is possible for the fibroblast fully commit to this phenotype and determine contractility based on the number activated in this way. A continuum of contractile activation might also be envisioned, where the average activation intensity and not cell density determines contraction.

Interestingly, we find that myofibroblast density does not directly correlate to CCN1 levels. Given that the observed capsule populations for Grade II and III had equivalent residing times, this is a paradoxical result. Myofibroblasts within the capsule appear to be a mixed population with different propensities to produce and respond to CCN1. It may be that a specific phenotype fibroblast differentiates in severe capsular contracture that is less sensitive to senescence cues like CCN1.[170] It is now known that there are a number of sources for fibroblasts including endoMT, pericytes, and circulating fibrocytes which may or may not make significant contributions in different wound healing scenarios.[171–174] It is possible that capsule fibroblasts are derived from one of these alternatives to a different extent than previously explored wound healing models. Additional markers such as Thy-1 would be useful to parse out these populations, as Thy-1 has been implicated in determining myofibroblasts vs lipofibroblastic phenotypes.[175] The Thy-1 promoter was shown to be hypermethylated in lung fibroblasts that generate fibrotic foci[176] which could support the hypothesis of matrix nucleation and growth presented here. To further elucidate the character of the capsule fibroblast, more detailed analyses of their phenotype and environment are needed.

In many ways, the region adjacent to the implant is the first line of interaction between the body and a foreign object. Previous work has demonstrated that the first 50-200μm from the implant surface forms a synovial membrane similar to those typical of joints. Despite an epithelial appearance, no basement membrane is present and the dense cell population is vimentin-positive fibroblast-like cells and CD68+ phagocytic cells.[135] The work presented here supports these findings and confirms a macrophage and fibroblast rich interface region roughly 200μm thick.
Macrophages are a key modulator of the wound healing environment and fibroblast phenotype via paracrine factors.[156,157,177] The work of Gordon et al developed a macrophage classification system which loosely separates macrophages into inflammatory (M1) or anti-inflammatory (M2).[178] A

number of difficulties have arisen as these groupings have been investigated in greater depth.[179] However, the designation still serves as a decent sign post from which to begin. Numerous markers have been associated with each phenotype and differ between mouse and human. In humans, CD163 positive macrophages have been implicated in the resolution of inflammation[180], while CD86 positive macrophages are associated with proinflammatory cytokines such as IL6, iNOS and IL-1β. [181,182] Data presented here suggests that macrophages associated with resolution are more important players in capsule severity because no difference in CD86 macrophages could be detected in any measure.

One notable product of macrophages is collagen VI.[183] The work presented here demonstrates a high density of macrophages at the implant interface along with a collagen VI dense region of matrix. This collagen VI region is curiously opposed to and just subjacent to, the highest density region of myofibroblasts. Naugle et al demonstrated that collagens I and III promote fibroblast proliferation while collagen VI is important for fibroblast differentiation in heart infarct.[184] It is possible these macrophages are using structural cues to inform myofibroblasts behavior or differentiation. Theocharidis et al demonstrated that collagen VI was expressed at the expanding margins of keloid scars and matrices generated without collagen VI were significantly thinner with thicker collagen fibers *in vitro*. Fibers.[162] The juxtaposition of the M2 collagen VI interface region with the myofibroblasts dense band suggests interesting prospects for future, more mechanistic, studies.

Clinically, a large range in capsule severity is seen between patients[124,149], and whilst there have been many studies of what may drive this variation, its molecular and cellular basis is poorly understood. Animal studies have been used to look at mechanism[36,136,185,186] but it is unclear how these studies correlate to the human breast cancer patient. For example, rodent models exhibit a foreign body response similar to humans, but require radiation to induce contracture, suggesting an aspect of contracture is unique to humans.

Interpretation of results from humans has also provided challenges. Studies in humans have been limited to clinical variables and tissues removed at the time of revision. Knowing the clinical aspects that relate to poor outcomes is in many ways most important to clinicians; however, it does

not provide a pathway to understanding mechanism or new, mechanistically based treatments. Additionally, waiting until the patient elects to have surgical revision prevents the collection of low grade capsules for comparison and creates a variation in capsule tissue age that is problematic.[131] Often variability between patients limits conclusive correlations.

Utilizing the more uniform tissue expander-derived capsules has demonstrated an improved ability to distinguish between capsule grades. Some work has demonstrated that capsules from dynamic silicone expanders are not equivalent to static silicone implants. [187] Other work has also suggested that expander-derived capsules are equivalent to static silicone implants when implant residing time is accounted for.[132] Adkinson et al suggested that complications with the tissue expander correlated to increased complications with the final implant, however, they do not link capsule grade. [133] Bui et al performed similar quantifications on a much broader range of capsules obtained from revisions of silicone implants. They found greater αSMA immunoreactivity in higher grade capsules, but no significant correlation between CD68+ cells and contracture status. Additionally, these workers utilized an alternative quantitation of capsule structure, fiber alignment, and found that fiber alignment increases with capsule grade.[131] All of these data are congruous with those found here, suggesting that our results at 3-4 months are indeed representative of long term outcomes.

Conclusions

Capsule tissue derived for tissue expanders are a viable model for capsular contracture that provide the best variable control outside of a laboratory. This model is able to reach significance in measures that only showed trends in previous work and has produced novel findings not feasible with other clinical models.

CHAPTER 4: Gene expression variance in relation to capsular contraction severity in women undergoing breast reconstruction following bilateral mastectomy

4.1 ABSTRACT

The study of capsular contracture has thus far relied on large sample sizes to tease out possible correlations to capsule severity, which limits the detail of the analysis both in manpower and assay cost. By using a highly standardized clinical model, we have previously demonstrated the ability to attain significance with a relatively modest, but sufficiently powered, sample sizes. By decreasing sample size, cost prohibitive techniques become possible. RNA-seq is one such tool that provides unprecedented depth of detail in differential expression. Building on differential expression results from RNA-seq, pathway enrichment allows high numbers of gene to be distilled into a biologically relevant context, which can be then used to identify novel biomarkers and targets for therapeutics. To this end RNA-seq was performed on 31 tissue samples from patients undergoing breast reconstruction following mastectomy. A paired differential expression analysis resulted in 1029 significantly dysregulated genes. Of those, 189 had greater than one log fold change. Pathway enrichment was then performed; highlighting IL4/13 signaling, extracellular matrix organization, antigen presentation, and interferon signaling as importantly dysregulated pathways. Differential expression results were also compared to various clinical and histological measurements to evaluate novel correlations. PVT-1, a long non-coding RNA oncogene, was strongly correlated to breast capsules formed after cancer removal. This suggests cancerous transformations of cell types that remain after the tumor is removed, such as cancer associated fibroblasts and macrophages. Furthermore, transgelin and caspase 7 were correlated to myofibroblasts density, suggesting the existence of an abnormal fibroblast phenotype that is resistant to apoptosis and may have enhanced contractile abilities. Capsule formation is a complex process however, with well controlled clinical models quantitative differences can be found. These results serve as stepping stone for the field to move beyond retrospective clinical trials and pursue mechanistically informed treatments and preventative measures.

4.2 INTRODUCTION

The body responds robustly to foreign objects embedded long-term, ranging from splinters to medical devices by encapsulating them in a dense collagen matrix. In the case of soft silicone implants, this enveloping capsule begins to contract around the device generating distortion, hardening and sometimes pain.[147,188] Capsular contracture is a common complication following breast reconstruction, with incidence rates ranging between 2 and 50% and typically requires additional surgery for correction.[20,189] This applies to breast enhancement for cosmetic reasons, but also for women undergoing reconstruction following prophylactic mastectomy because of risk cancer or reconstructive surgery following remission from breast cancer. In the latter case, it widely held that the prospect of more severe capsular contracture is increased owing to aggravating factors such as radiotherapy, chemotherapy and loss of axilliary lymph nodes in association with cancerous tissue removal.[20,153,189,190] The exact cause(s) of capsular contracture are unknown, but many attempts have been made to understand clinical and histological variables that impact contracture severity.[34,131,135,191–193]

To date, the study of capsular contracture has largely involved clinical studies and histological analyses. The understanding of gene expression patterns and genetic pathways associated with variance in severity of capsular contracture has been relatively limited.[30,169,194] RNA-seq is a powerful tool that if used judiciously can lessen preconceptions from the selection of variables, providing relatively unbiased surveys of gene expression profiles potentially encompassing the entire genome. While often criticized for its overabundance of findings, when properly applied RNA-seq is a tool to identify new paths of study.[195–197] Building on differential expression results from RNA-seq, pathway enrichment examines genes that are significantly different between two groups and asks if more genes from the set are associated with a particular pathway than would be expected by chance.[198–200] This approach allows high numbers of gene reads to be distilled into a biologically relevant context, which can be then used to identify novel biomarkers and targets for therapeutics.

RNA-seq is still relatively cost prohibitive. Previous work has relied on large sample sizes to offset large variability within the sample. The application of more sensitive quantitative technique

requires greater control of clinical variables so that meaningful results can be obtained. This study utilized capsule tissue derived from temporary saline-filled silicone shell expanders that were surgically placed to prepare the reconstruction site for the final implant. This approach allowed for a relatively narrow time window to be examined across a uniform implant type. Pathologic responses were further controlled by normalizing to a group of Baker Grade I capsules, the ideal implant response. Here, we identify genes and pathways that vary between capsules of different severity during the initial 3 to 4 months of formation of this specialized type of internal scar tissue. In particular, we interrogate genes and pathways contributing to severity of capsular contraction within patients undergoing bilateral mastectomies and between patients. These data may provide insight into the role of environmental versus inherent genetic factors in this pathology.

4.3 MATERIALS AND METHODS

Sample collection

In order to evaluate a more uniform time point, samples were taken from silicone expanders at the time of exchange. Tissue was collected, dissected free from excess fat and muscle tissue, and placed directly in RNAlater (ThermoFisher SKU#AM7021) storage solution in the operating room. Samples were allowed to saturate for 24 hours at 4°C and weighed and stored at -80°C. RNA was isolated by pulverizing the tissue and extraction in Trizol. Samples were then purified using Micro to Midi RNA Purification columns with DNAse treatment. Only samples with RIN greater that 8 were used in this study. Patients were selected in order to eliminate as many confounding factors as possible (Table 4.1). Additionally, only bilateral reconstructions were utilized to provide the option of within patient comparisons.

	Grade I	Grade II	Grade III
Age	59.3	45.8	48.3
Implant Residing Time	4.0	3.4	4.0
Chemotherapy	0.0%	69.2%	78.6%
Radiation	0.0%	7.7%	28.6%
Diabetes	0.0%	0.0%	14.3%
Smoking	0.0%	0.0%	7.1%
n=	3	14	14

Table 4.1 RNA-seq Patient Cohort RNA-seq was run on 31 capsules, 29 were included in the final analysis. One pair was excluded due to its status as a statistical outlier, more detail in patient data is needed to determine the cause of the disparate expression.

Library Prep and Sequencing on Illumina 2500

All the RNA-Seq work was performed at the Virginia Tech Biocomplexity Institute's Genome Sequencing Center. All the library preps are performed on Apollo 324 Robot (Wafergen, CA). 500 ng of total RNA with RIN ≥ 7.0 was enriched for polyA RNA using PrepX PolyA mRNA Isolation Kit (P/N 400047, Wafergen, Fremont, CA). Poly(A) RNA was then converted into a library of template molecules using PrepX RNA-Seq for Illumina Library Kit, 48 samples (P/N 400046, Wafergen, Fremont, CA) for subsequent cluster generation and sequencing by Illumina HiSeq. The libraries were purified and enriched with 13 cycles of PCR to create the final cDNA library. The 280-300bp libraries (160-180 bp insert) generated were validated using Agilent 2100 Bioanalyzer and quantitated using Quant-iT dsDNA HS Kit (Invitrogen) and qPCR. Individually indexed libraries were pooled and sequenced on Illumina HiSeq 2500 Rapi Run, to 1x 101 SR cycles using two TruSeq Rapid SBS Kit (50-cycles) (FC-402-4002). One patient's RNA was included in all runs as a reference sample for analysis purposes.

Differential Expression Analysis

Following sequencing, data was trimmed for both adaptor and quality using a combination of ea-utils and Btrim.[201,202] Sequencing reads were then aligned to the genome using Tophat2/Bowtie2[203] and counted via HTSeq.[204] QC summary statistics were examined to identify any problematic samples (e.g. total read counts, quality and base composition profiles (+/- trimming)), raw fastq formatted data files, aligned files (bam and text file containing sample alignment statistics), and count files (HTSeq text files). Following successful alignment, mRNA differential expression was determined using contrasts tested for significance using the Benjamini-Hochberg corrected Wald Test in the R-package DESeq2.[205]

Pathway enrichment

Genes with p values below 0.05 were compiled into gene lists, distinct for each differential expression comparison. The gene lists were then analyzed with Reactome[200,206] pathway enrichment. Pathway enrichment looks at the list of significant genes and evaluates if more genes from a given pathway are present than would be expected in a random list. A p-value is calculated for the enrichment as well as a false discovery rate (FDR). Only pathways with both a p value and FDR less than 0.05 were considered significantly enriched.

4.4 RESULTS

Analysis Rationale

Patient sequencing results were compared in several ways (Figure 4.1). The first was what we termed the unpaired analysis, which disregarded patient anonymized identifier number (ID) as a factor in the analysis (Figure 4.1a). The intent of the unpaired analysis was to provide a population analysis more similar to previous work in the field. The aim was to determine common genes or pathways influencing capsule severity across patients. Numerous pathways are commonly upregulated in a wound healing or foreign body response; yet, to determine which are pathological those normal pathways need to be accounted for. To do this, contraction capsules of Grades II and III were normalized to Grade I capsules. Results are presented as Grade III with respect to Grade II. Second, patients that had two samples, one from each breast, were then analyzed as paired samples to distinguish differences between Grade II and III in asymmetric patients (Figure 4.1c).

In doing this, patient-to-patient variation is removed from the comparison, leading to the cleanest differentiation of gene expression changes between Grades II and III that were common in the patients studied. The third grouping disregarded grade and compared symmetric patients to asymmetric patients in order to shed light on the genes and pathways that trigger asymmetry at the clinical level (Figure 4. 1b).

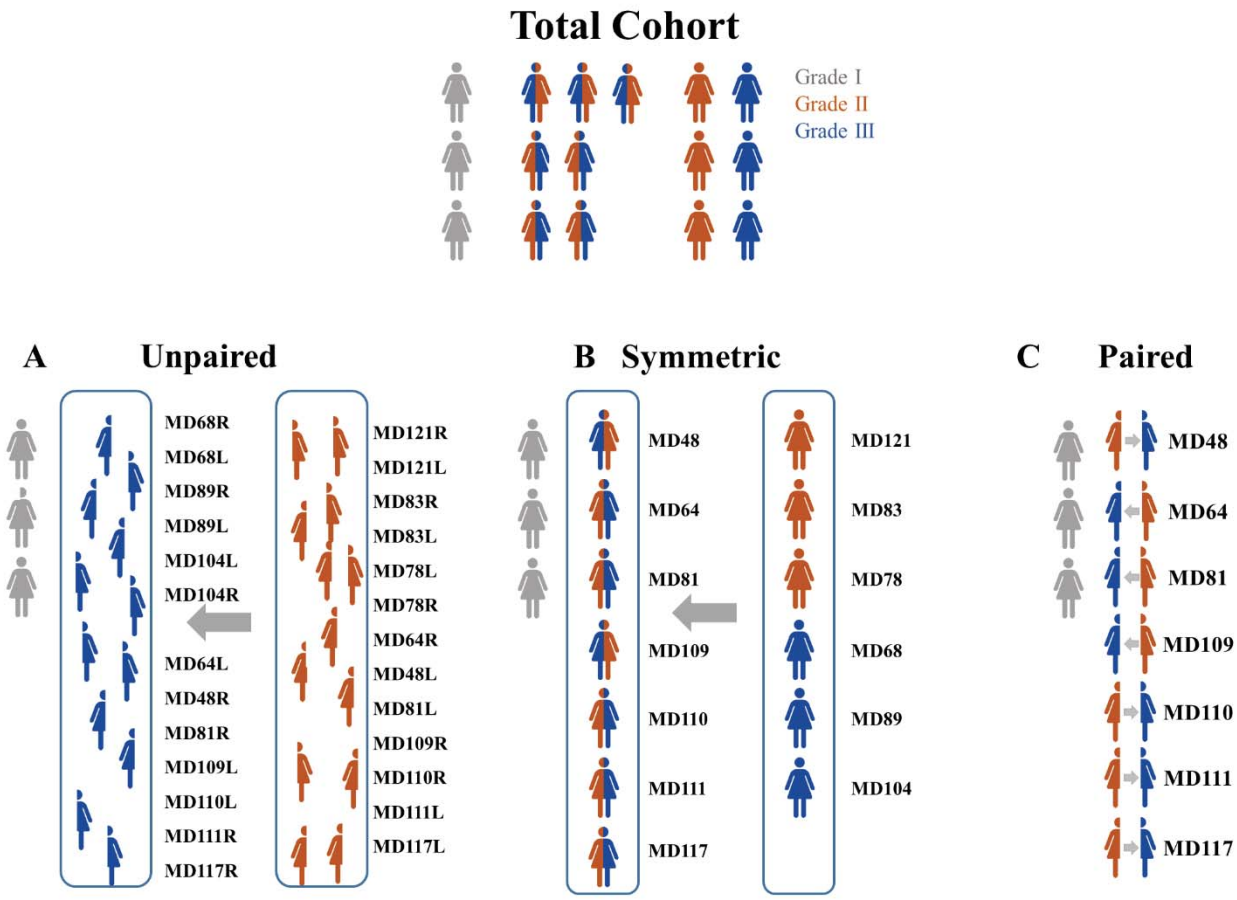

Figure 4.1. Rationale for RNA-seq Analysis Capsule tissue was collected from 16 patients, three grade 1 capsules from 3 individuals, 14 capsules from 7 asymmetric individuals, and 12 capsules from 6 symmetric individuals. Patients were assigned ID numbers of the format MDXX with left or right side denoted by L or R (e.g., MD25R is patient 25's capsule from the right side).The grade I capsules were used as a control group to normalize all grade II and III capsules. Grade I results were not considered on their own in this analysis. The capsules were subdivided in three ways A) all grade II capsules were compared to all grade III regardless of the patient identification to evaluate across patient variation, B) capsules from asymmetric patients were compared to symmetric patients to identify genes associated with asymmetry and C) Grade II capsules from asymmetric patients were compared to their matched grade III in order to look at within patient variation and reduce the impact of patient to patient variability.

Unpaired results

When Grade II and III capsules were compared in an unpaired fashion, 95 genes were found to be significantly different. Eight of those genes were greater than 1 logfold change: Haptoglobin (HP), Zinc finger and BTB binding domain containing 16 (ZBTB16), RAS Dexamethasone-Induced 1 (RASD1), SHC Binding And Spindle Associated 1 Like (SHCBP1L), CCAAT/Enhancer Binding Protein Delta (CEBPD), Mitochondrially Encoded NADH:Ubiquinone Oxidoreductase Core Subunit 1 (MTND1P23), and RNA Binding Protein With Serine Rich Domain 1 Pseudogene 1 (RNPS1P1) were upregulated in grade three capsules while a non-protein coding RNA, AL139352.1 was down regulated.

HP is a salvage receptor that binds free hemoglobin released from platelets to inhibit its oxidative activity and can inhibit collagen degradation.[207,208] HP expression was highly enriched in Grade III capsules (3.17 lfc), and as its presence is correlated with hemoglobin, it may suggest the possibility that ongoing bleeding causes increased contracture severity in some of the patients.

Paired results

Comparing Grade II and III capsules from patients with asymmetric capsular contracture on their left vs right side yielded more significant genes. Patient ID was found to be a significant contributor to variation meaning that the variation between people is large enough to overwhelm smaller differences seen between grades. 1044 genes were significantly different; 302 were down regulated and 740 were upregulated in Grade III capsules compared to their Grade II pair. Of those, 183 were differentially regulated by more than 1 logfold up or down. 63 of these genes were related to muscle, including, intriguingly, numerous cardiac muscle genes. Numerous non-coding RNAs were also found to significantly vary between paired Grade II and III capsules, which is of particular interest due to the recent recognition that these molecules may have key roles in regulating expression of genes and suites of genes.[209–211] Additionally, a large numbers of different MHC classes were dysregulated in Grade III capsules. Some of these MHCs have been shown to vary in keloid and hypertrophic scars.[122,199]

IL-1b and IL1RN operate in competition for the same receptor. Both genes are upregulated to the same extent though the ratio was highly skewed towards IL1RN, with 3.8 and 2.7 times more IL1RN than IL1B in Grades II and III respectively (ratio difference between grades p=0.17). This suggests that in both grades a strong opposition to IL1b is present, slightly more so in grade 2. Interestingly, IL1R2, a decoy receptor for IL1b[212], is expressed at a lower level than IL1RN but is slightly upregulated in Grade III capsules. It's possible that Grade III capsules employ a different mechanism of IL1 silencing.

Symmetric vs asymmetric

When grade was disregarded. 12 genes differed significantly between symmetric and asymmetric capsules, 10 of which were greater than 1 logfold different. Bromodomain containing 2 (BRD2), Cholinergic receptor nicotinic alpha 10 (CHRNA10), family with sequence similarity 153 member A (FAM153A), RFPL3 antisense (RFPL3S), leukocyte immunoglobulin like receptor B2 (LILRB2), Lactate Dehydrogenase C(LDHC), BACE1 antisense RNA (BACE1-AS), serine/threonine kinase 2 (SGK2), and mitochondrially encoded tRNA tryptophan (MT-TW) were upregulated in asymmetric patients while syntrophin gamma 1 (SNTG1) was down regulated. LILRB2 is of particular interest in this list because it is expressed largely on immune cells. It binds to MHC-1 on antigen presenting cells and transduces a negative signal to suppress stimulation.[213]

Clinical and Histological Variables	Correlated Genes												
Collagen Maturity	KRTCAP2	TMEM205	AC013472.1	AC015574.1	RASA4B	TSGA10IP							
Matrix Entropy	PDP1	AL450326.1	DENR	CSNK2A1	NAXD	ASPH	SMG6	AC084855	HBS1L	OSTF1	CDC16	GGA3	
	TMEM230	MRPS10	LACTB2	MZT1	KCTD12	UCHL5	GDI1	MIR3671	SNX2	HDLBP			
Tissue Thickness (um)	NMU	COL17A1	C3orf36	STK38	HLA-DPB1	AC002550.1	SHOX	FOXD4L1					
Interface Thickness (um)	HLA-DRB5	CDH24	MIR210HG	CLSTN3	NOTCH3	TMEM132A	JAG2	CACNA1I	LINC00922	LRRC7I	DIO3OS	AC020763.4	AP003040.1
	LPAR2	ARL6IP1	PPP1R14A	AEBP1	ERFE	OXER1	CDC42EP	TPSAB1	CPLX1	TINAGL1	ACTA2	AC008694.2	GNG8
	MIOS	ATP6V1D	AC005306.1	CCL21	ICAM4	SSUH2	DPYS	TRIM56	AL049569.1	GIPR	AP000146.1	AC120498.10	HMOX2
	WWC1	CNN1	SBSN	CXCL12	GLIS1	DIO3	PCED1A	ZFHX2-A	SLC39A4	LMOD1	TMIGD2	FAM46B	AP000897.2
	AC010491.1	TSPAN9	NDUFV2	BPIFB1	SCIN	DOPEY1	PHRF1	AC073335	AC026461.3	PLGLA	AC134050.1	SDCBPP2	RASL11A
	SLC9A3R2	ARMC12	OR51E2	AC009299.2	GSTT2	LINGO1	VPS9D1-/	S1PR5	WFDC2	ITIH3	TLE6	GUCA1A	AC111182.1
	LDOC1	CCDC97	KCNA5	HRCT1	AL391121.1	BCYRN1	AL390037	AP001029	AC046168.2	LINC01186			
Vessel Density (F)	EIF3C	WNT16	AP000757.1	RPL5	ABCA10	SELENOS	KIF12	PRSS12	AC105411.1	NECTIN4	HCRTR1	AC026333.4	DNAH11
	AC105052.3	AC020718.1	ZNF251	SNRPGP10	AC007249.1	ABCA9	LINC01160	HIST3H2I	AC009090.4	NUTM2HP			
Mean Vessel Size (um)	SCRG1	AC098829.1	MRPL45	RNF175	SEMA3A	DANT2	GRIK4	LINC01487	ZNF730	LINC02507	AC011247.1	AC092167.1	AP002026.1
	ZNF98	AADACL2-A	CMSS1	ZNF461	NIPAL2	LENG8-AS1	LINC00684	GRID2	OR7D2	GTF2IP5	AC003684.1	AL590762.2	AC010378.1
	C11orf87	PTCHD1	AC018709.1	PIGL	AL356599.1	POLR2J4	AC106760	CHURC1-1	CERK	SLC39A11	LINC01579	AC022398.1	AC106754.1
	AZIN1-AS1	CCNYL2	ZNF30	GRAMD2B	ST18	PTENP1-AS	DNAH14	TMEM244	AL117339.1	DACT3-AS1	RPP30	LINC02211	AC091946.1
	SNORA11F	LINC00276	FAM133A	RAB30	GULOP	AC008758.4	C21orf62-A	VWA3B	AC090282.1	ZNF90	PTPRG-AS1	LINC01925	RNA5SP352
Activated Fibroblasts Density	TAGLN	RASSF2	PER1	PLCL2	ART4	CASP7	SLC38A4	AL590235	ANKHD1	AC135050.3	C6orf99	RIMKLBP1	
CCN1 Integrated Density	NMU	UNC5CL	AL049844.1										
Fibroblast: Vascular Smooth Muscle aSMA	PYGM	ENO3	SEMA3G	C10orf10	PGAM2	KRT16	DTX4	COX6A2	NOS1	FBP2	SPP1	LINC00578	MAP3K7CL
	MESP1	LINC02345	AL591806.3	ZBTB16	STMN2	EPYC	AC066613	SCN2A	NXPH4	NEURL1	AC007325.4	AC096577.1	AC012555.1
	LINC02082	FCGR1A	LCMT2	LINC00092	AC091563.1	AC010980.2	AF127936	PKP4-AS1	AC092384.2	ANXA8	CLLU1OS	Z84484.1	AC092378.1
	NDUFAF1	HIST2H3D	AC092757.2	AC087239.1									
Cancer	PVT1	AL390729.1											
Patient Age	IFI44L	CMPK2	AL139125.1	LRRFIP2	CLEC18A	CREB3L3	AC010615	IFIT3	EPHX2	ANKK1	IFIT2	LILRA4	OAS1
	LINC01235	FAM157C	CH13L2	AC092683.1	PCGF3	TACR1							
Implant Residing Time	C17orf97	ABCA4	NPIPA5	SPATA32	PIGBOS1	GALT	PRSS8	DSTNP1					
Right	LINC00444	AC091814.1	AL109653.1										
Left	LINC00444	AC091814.1	AL109653.1										
Chemotherapy	GTF2H2	GTF2H2B	AL512625.3	LINC02470	RNASEH2B-A	NBPF3	KIAA1671	RPL39	IGHG4	AC138969.2	LINC00476	AC036176.1	AC104248.1
	GUSBP9	AC106882.1	PCDHB10	SMIM11A									
Radiation	STOX1	CALHM6	ANKRD22	GNLY	AC135983.2	GBP5	CXCL9	KLRC1	ANO4	ALDH9A1	MIR4300HG	NOP10	TBC1D14
	DOPEY2	TDRKH	IFNG	YPEL1	RPL39P5	SYK	RAD51-A	KLHL10	AC004921.1	TNS4	ZNF683	OGFRP1	AC133485.3
	SMIM2-AS1	LPIN1	CXCL10	LACTB	LINC02506	CXCL11	SYNE2	NBPF9	CSPG5	NBPF19	AL121761.2	FNTB	TMEM202-AS1
	AL390066.1	ACPP	ARL4A	SNX1									

Table 4.2 Gene Expression Results correlate to clinical and histological findings. Genes were screened for a correlation coefficient of 0.8 to each histological variable.

Clinical and Histologic Context

Expression results were then compared to clinical and histological variables in the same cohort of patients (Table 4.2). For this analysis, the complete expression profile was used, not just the genes significantly different between Grades II and III. Correlation coefficient threshold was set to 0.8 in order to identify meaningfully elevated relationships, but produce a manageable set of correlations for evaluation.

The presence of cancer strongly correlated to the expression levels of PVT-1, a long non-coding RNA down stream of myc known to be an oncogene. PVT-1 is largely found in transformed cells so its continued presence in "normal" tissue implies continued influence of cancer in the wound healing environment long after its removal. CCN1 gene expression and protein level expression were tightly correlated and additionally correlated to the thickness of the cell dense region interacting with the implant.

Additionally, myofibroblasts (Vimentin+/αSMA+ cells) correlated to transgelin and caspase 7. Transgelin is a shape change and transformation sensitive actin binding protein that is ubiquitously expressed in vascular and visceral smooth muscle. Interestingly, myofibroblasts density positively correlates to capsule grade but there is no difference in the ratio of myofibroblasts to vascular smooth muscle cells across capsule grades. Caspase 7 is negatively correlated to myofibroblasts density, suggesting greater density of myofibroblasts is the result of impaired apoptosis.

Pathway Enrichment

Pathway enrichment utilizes a large, curated database of gene relationships and known pathways to determine connections within a given dataset.[198,200] A gene list is created from the significant genes in a differential expression analysis, this list is then cross referenced to the database. The analysis asks: are there more genes from a given pathway in the gene list than would be expected by random chance. Going forward, only the paired differential expression results will be used because the other comparisons resulted in too few genes for meaningful pathway enrichment. Reactome was used to identify 39 pathways that were significantly enriched in the paired Grade II and III comparison, as determined by both a p value and a false discovery rate below 0.05 (Table 4.3).

The antigen processing and cross presentation pathway was enriched with 75 pathway genes found in the gene list. Sub-pathways that were also significant include: folding assembly and peptide loading of class 1 MHCs, Class I MHC mediated antigen processing and presentation, and the ER-phagosome pathway. Genes included the HLA genes as well as ERAP1 and 2, PSMB6, CD14 and CD36. Fifteen pathways involving eukaryotic translation were also enriched. Various ribosomal subunits constitute the pathway genes represented in the gene list.

Cytokine signaling in the immune system was also enriched based largely on the sub-pathways of Interferon signaling and IL4/13 signaling. Beyond HLA molecules, ICAM1, NCAM1, IRF1 and OAS3 contribute to the interferon pathway. IRF1 is slightly, but significantly down-regulated in Grade III capsules. IRF1 is associated with the activation of MHC class I and II expression, TNFSF10 and interleukins 7 12 and 15 and the repression of FOXP3, IL4 and the maturation of dendritic cells and T-reg development.[214–217] OAS3 is an interferon induced antiviral agent that may also play roles in apoptosis and differentiation[218], made additionally interesting by the significant enrichment of the viral mRNA translation pathway.

Il-4 and 13 signaling were also enriched in this gene list with 37 of 212 genes in the pathway represented ($P<0.01$ FDR=0.004). Of those, 13 were products that should be upregulated, only fibronectin was down regulated; yet, none of the products that would be expected to be downregulated were found to be. IL 4 and 13 are produced by Th2 cells and early mast cells around foreign objects and stimulate the M2 polarization of macrophages that promote wound healing, or in some cases, fibrosis.[219] Moyer et al demonstrated that Grade II capsules had more mast cells than Grade III counterparts at a similar time point to the present study[31]. Also in this pathway, BCL6, responsible for the B-cell response to IL-4[220] as well as the differentiation of naïve helper T cells into follicular helper T cells[221], is upregulated.

4.4 DISCUSSION

In this study we provided an overview of gene expression patterns associated with variance in capsular contracture in a highly controlled clinical model. Our unpaired analysis identified genes associated with excess bleeding (HP) and bacterial infection (LBP) which were strongly upregulated in Grade III capsules compared to Grade II. By accounting for patient-to-patient variability, the paired analysis identified differences in the immune profiles. Pathway enrichment of the paired analysis suggests more specific differences in interferon and IL-4/13 signaling as well as antigen presentation.

Kyle et al performed a microarray analysis of capsule tissues and compared uncontracted versus contracted capsules. Their study included 23 capsules from patients undergoing implant removal or exchange, 13 of which were post-mastectomy reconstruction. Implants were either silicone or saline filled, smooth or textured, and most were placed sub muscularly. The average residing time was 6 years, though the control group averaged 5 years, while the contracted group averaged 9 years. They found 257 dysregulated genes and selected 6 genes based on magnitude of dysregulation for further study. Aggrecan, TIMP4 and TNFSF11 were down regulated while MMP12, SAA1 and IL-8 were upregulated. They validated these targets with both PCR and immunohistochemistry. Only IL-8 and TIMP4 were validated by all three measures.[33]

The study of Kyle and co-workers[33] is most congruent in structure to the unpaired results presented here. Similar trends for MMP12, TNFSF11 and SSA1 identified by these authors were found in our study but they did not reach significance. TIMP4 was upregulated very slightly and IL8 was not detected. With such different residing time windows, this is a reasonable degree of similarity. The differences that were observed can potentially be explained by the current study's focus on post mastectomy patients, which are known to have more inflammation. The inclusion of cosmetic procedures in Kyle et al's work likely mitigated the levels of inflammation associated with the more extreme reconstructions investigated in our study.

Wolfram and colleagues[37] performed a flow cytometry analysis of the lymphocytes found within 37 capsule tissues. Capsules were largely derived from cosmetic procedures, with either

subglandular or submuscular placement. They found that CD4+ cells predominated with a higher proportion of capsule T cells expressing γ/δ receptors than their peripheral blood counterparts. An inverse correlation was found between the number of T-reg cells and the severity of the capsule. Interestingly, the suppressive capacity of T-regs from higher grade capsules was reduced. IL6, IL8, IL17, TGFβ and IL1B were detectable in supernatant from isolated cells. They suggest that it is not only reduced numbers of T-regs, but also a reduced quality that leads to more severe contracture.[37]

The present study supports the findings of Wolfram et al [37] with increase IL6 and IL1B in higher grade capsules and an overall high TGFβ expression level. Further comparisons are difficult because of the difference in controls, peripheral blood and Grade I capsules. This study did not find that γ/δ receptors were upregulated and was unable to detect a difference in IL17 or IL8 transcripts. Additionally, differences were detected in the IL4/13 pathway including the upregulation of BCL6, which could suggest Tfh cell formation, yet CXCR5 is reduced but not to significance[222,223]. Other genes associated with Tfh cells[224] are present in the current study, however their low expression levels make conclusions difficult. Analyzing full tissue mRNA profiles seems to have limited detection of genes or pathways from small subsamples of cells in this data set.

Interestingly, only 10 genes were found in common between the paired and unpaired analysis; of particular interest were insulin receptor substrate 2 (IRS2), CEBPB, RAN binding protein 3 like (RANBP3L), FK506 Binding Protein 5 (FKBP5), and Growth arrest and DNA-damage-inducible protein GADD45 gamma (GADD45G). CEBPD is a CCAAT enhancer-binding protein with known functions in tissue differentiation and the immune response. CEBPD is largely expressed in eosinophil and monocyte lineages and in certain phases of T cell differentiation.[225] It has also been implicated in adipogenesis but this property can be ameliorated via TGFβ signaling through Smad 3.[226,227] It was also demonstrated that TGFβ induces CEBPD in pancreatic stellate cells which activates HIF-1a and contributes to anti-apoptotic and pro-fibrotic conditions[228]. Duitman et al demonstrated that deficiencies in CEBPD enhanced fibrosis in the kidney in mice.[229] CEBPD's impact on fibrosis is highly context dependent and further work is needed to tease out

the results reported here, namely that Grade III capsules have significantly more CEBPD than Grade II capsules.

By correlating gene expression to clinical variables an interesting picture begins to emerge. Capsule severity positively correlates to myofibroblasts and CCN1 expression (Chapter 3). CCN1 is a negative regulator of myofibroblast differentiation, inducing apoptosis in dermal fibroblasts[164,165]; meanwhile, synoviocytes, fibroblast-like cells in cartilage, receive a feed-forward signal from CCN1 to increase proliferation.[230] In this scenario, apoptosis may be inhibited as evidenced by caspase 7 expression while capsule fibroblasts are also lacking inhibition from CCN1. Combining these results with the unpaired analysis, one hypothesis is that fibroblasts in Grade III capsules have been activated differently and are functioning more like synoviocytes, than the more traditional idea of a myofibroblasts. Ongoing studies might focus on whether such cells are uniformly distributed through the capsule, or more focally e.g., at the implant-tissue interface. Bleeding in the implant pocket could be a factor accounting for the increased expression of haptoglobin in higher grade capsules, creating a microenvironment similar to macroscale hematoma, which has regularly been associated with poor reconstruction outcomes.[20,189]

This work is limited by its RNA focus. Protein expression and regulation are not always related to transcript levels. Several genes, CD163, CD86, CD68, iNOS, ARG1, CYR61, CD4, CD8, Collagens I III and VI, and αSMA were checked with qPCR and found to match trends and detection limits seen in the RNA-seq data. Additionally, immunofluorescence confirmed for CD163, CD86, CD68, CYR61, Collagens I III and VI, CD31 and αSMA. While these genes matched well across data sets, it does not speak for the whole data, set as proteins such as TGFβ require proteolytic cleavage for activation and alternatively can be sequestered by binding to matrix proteins. Further work is needed to build from these findings.

Conclusions

When RNA-seq is applied to a controlled clinical model, unprecedented detail of the differential gene expression and enriched pathways found in severe capsular contracture is illuminated. Between-patient variability proved a large contributor to differences in expression so a paired analysis, utilizing samples from patients with asymmetric capsule grades, was performed. When validated these results can be used to better understand the driving pathways of capsule severity and explore novel drug targets to mitigate those pathways.

Pathway name	Pathway identifier	#Entities found	#Entities total	Entities pValue	Entities FDR	Submitted entities found
Antigen Presentation: Folding, assembly and peptide loading of class I MHC	R-HSA-983170	74	102	1.11E-16	1.91E-14	HLA-H;ERAP2;ERAP1;HLA-B;HLA-C;HLA-A;HLA-F
Endosomal/Vacuolar pathway	R-HSA-1236977	72	82	1.11E-16	1.91E-14	HLA-H;HLA-B;HLA-C;HLA-A;HLA-F
ER-Phagosome pathway	R-HSA-1236974	75	164	1.11E-16	1.91E-14	PSMB6;HLA-H;HLA-B;HLA-C;HLA-A;CD14;CD36;HLA-F
Antigen processing-Cross presentation	R-HSA-1236975	75	186	1.11E-16	1.91E-14	PSMB6;HLA-H;HLA-B;HLA-C;HLA-A;CD14;CD36;HLA-F
Immunoregulatory interactions between a Lymphoid and a non-Lymphoid cell	R-HSA-198933	95	316	1.11E-16	1.91E-14	IGHV1-2;IGHV3-23;ICAM3;ITGAL;TREM1;IGLV4-60;ICAM1;IGLV2-8;IGLV1-47;KLRC4-KLRK1;IGLV1-44;HLA-H;IGLC7;IGKV2D-40;CD300A;HLA-B;HLA-C;ULBP2;HLA-A;HLA-F;CLEC2B;SELL;FCGR2B;IGLV3-19;CLEC4G
Interferon gamma signaling	R-HSA-877300	95	176	1.11E-16	1.91E-14	CAMK2B;HLA-DRB5;HLA-H;HLA-B;HLA-C;HLA-A;HLA-F;ICAM1;IRF1;OAS3;NCAM1;HLA-DQA1;HLA-DRB1;HLA-DQB1
Interferon Signaling	R-HSA-913531	96	292	1.11E-16	1.91E-14	CAMK2B;HLA-DRB5;POM121;HLA-H;HLA-B;HLA-C;HLA-A;HLA-F;ICAM1;IRF1;OAS3;NCAM1;HLA-DQA1;HLA-DRB1;HLA-DQB1
Interferon alpha/beta signaling	R-HSA-909733	74	141	1.11E-16	1.91E-14	HLA-H;IRF1;OAS3;HLA-B;HLA-C;HLA-A;HLA-F
Cytokine Signaling in Immune system	R-HSA-1280215	168	961	1.35E-13	2.06E-11	IL1RN;CSF3R;PTPN2O;F13A1;CXCL1;IRS2;FGF2;ICAM1;GHR;IGHG1;CCND1;PPP2R1B;RPS6KA2;LBP;CD36;CCR5;MEF2C;HLA-H;MMP1;HGF;MMP3;HLA-B;HLA-C;LIFR;HLA-A;HLA-F;HCK;IL1B;OAS3;IRF1;RHOU-S100A9;HLA-DQB1;CAMK2B;LAMA5;POM121;MAQA;FPR1;TNFRSF11B;CSF2RB;PSMB6;CCL2;NCAM1;HLA-DQA1;IL12RB2;IL32;HLA-DRB5;CCL22;TNFSF14;IL34;FN1;IL31RA;SOD2;S100B;BCL6;IL2RA;PTPN5;HLA-DRB1;CRLF1
Striated Muscle Contraction	R-HSA-390522	23	40	2.63E-11	3.63E-09	TMOD1;MYBPC1;MYBPC2;ACTN3;ACTN2;TNNC1;TNNC2;NEB;TTN;ACTA1;ACTC1;DES;TNNT1;MYL1;MYL2;MYL3;TNNT3;TNNI1;TNNI2;TCAP;DMD;MYH7
Muscle contraction	R-HSA-397014	52	216	4.78E-09	5.97E-07	RYR1;TRIM72;DYSF;ATP2A1;RYR3;SLN;TMOD1;MYBPC1;MYBPC2;ACTN3;ACTN2;TNNC1;TNNC2;ITGA1;TRDN;ACTA1;TNNT1;MYL1;MYL2;TNNT3;MYL3;CASQ2;SCN4A;CASQ1;TUNI;MYH7;CAMK2B;KCNE1;ATP1A2;TTN;CACNG6;PLN;TNNI1;TNNI2;DMD;CACNA1S;CACNG1;CAV3;KCNIP2;KCNIP4;NEB;SORBS1;HIPK2;MYLPF;ACTC1;FGF14;DES;TCAP;KCNK3;SCN2B
Class I MHC mediated antigen processing & presentation	R-HSA-983169	83	464	1.16E-07	1.34E-05	HLA-H;TRIM63;ERAP2;FBXO27;ERAP1;HLA-B;UBR4;HLA-C;HLA-A;HLA-F;PSMB6;RNF144B;TRIM9;ELOB;CD14;CD36
Phosphorylation of CD3 and TCR zeta chains	R-HSA-202427	19	45	1.65E-07	1.75E-05	HLA-DRB5;HLA-DQA1;HLA-DRB1;PAG1;HLA-DQB1
Eukaryotic Translation Elongation	R-HSA-156842	30	104	2.33E-07	2.28E-05	RPS9;RPL30;EEF1A1P5;RPL21;RPS8;RPL34;RPL12;RPL35A;RPL23A;RPS3A;RPL3L;RPL7;RPS4X;RPS14;RPS27;RPL18AEEF1A2;RPL13;RPL27;RPL37;RPS10;RPL39;RPS12;RPS23
Translocation of ZAP-70 to Immunological synapse	R-HSA-202430	18	42	2.79E-07	2.57E-05	HLA-DRB5;HLA-DQA1;HLA-DRB1;HLA-DQB1
PD-1 signaling	R-HSA-389948	18	45	7.39E-07	6.36E-05	HLA-DRB5;HLA-DQA1;HLA-DRB1;HLA-DQB1
Peptide chain elongation	R-HSA-156902	28	99	8.44E-07	6.84E-05	RPS9;RPL30;RPL21;RPS8;RPL34;RPL12;RPL35A;RPL23A;RPS3A;RPL3L;RPL7;RPS4X;RPS14;RPS27;RPL18A;RPL13;RPL27;RPL37;RPS10;RPL39;RPS12;RPS23
Formation of a pool of free 40S subunits	R-HSA-72689	29	106	1.04E-06	7.90E-05	RPS9;RPL30;RPL21;RPS8;RPL34;RPL12;RPL35A;RPL23A;RPS3A;RPL3L;RPL7;RPS4X;RPS14;RPS27;RPL18A;EIF3CL;RPL13;RPL27;RPL37;EIF3C;RPS10;RPL39;RPS12;RPS23
Nonsense Mediated Decay (NMD) independent of the Exon Junction Complex (EJC)	R-HSA-975956	28	101	1.23E-06	8.88E-05	RPS9;RPL30;RPL21;RPS8;RPL34;RPL12;RPL35A;RPL23A;RPS3A;RPL3L;RPL7;RPS4X;RPS14;RPS27;RPL18A;RPL13;RPL27;RPL37;RPS10;RPL39;RPS12;RPS23
Laminin interactions	R-HSA-3000157	14	31	3.16E-06	2.18E-04	LAMA5;LAMA2;LAMB3;LAMA1;ITGA1;LAMB1;LAMC2;LAMC1;HSPG2;COL4A2;COL4A1;COL4A4;COL4A3;ITGA7
Viral mRNA Translation	R-HSA-192823	29	113	3.52E-06	2.29E-04	RPS9;RPL30;RPL21;RPS8;RPL34;RPL12;RPL35A;RPL23A;RPS3A;RPL3L;RPL7;RPS4X;RPS14;NA;RPS27;RPL18A;RPL13;RPL27;RPL37;RPS10;RPL39;RPS12;RPS23
Eukaryotic Translation Termination	R-HSA-72764	28	108	4.28E-06	2.65E-04	RPS9;RPL30;RPL21;RPS8;RPL34;RPL12;RPL35A;RPL23A;RPS3A;RPL3L;RPL7;RPS4X;RPS14;RPS27;RPL18A;RPL13;RPL27;RPL37;RPS10;RPL39;RPS12;RPS23
L13a-mediated translational silencing of Ceruloplasmin expression	R-HSA-156827	29	118	7.87E-06	4.72E-04	RPS9;RPL30;RPL21;RPS8;RPL34;RPL12;RPL35A;RPL23A;RPS3A;RPL3L;RPL7;RPS4X;RPS14;RPS27;RPL18A;RPL13;RPL27;RPL37;EIF3C;RPS10;RPL39;RPS12;RPS23
Non-integrin membrane-ECM interactions	R-HSA-3000171	19	61	1.28E-05	7.29E-04	LAMA5;LAMB3;LAMA2;LAMA1;ACTN2;FN1;TNC;LAMB1;LAMC2;LAMC1;FGF2;HSPG2;THBS1;COL4A2;COL4A1;COL4A4;COL4A3;COL10A1;DMD
GTP hydrolysis and joining of the 60S ribosomal subunit	R-HSA-72706	29	122	1.44E-05	7.93E-04	RPS9;RPL30;RPL21;RPS8;RPL34;RPL12;RPL35A;RPL23A;RPS3A;RPL3L;RPL7;RPS4X;RPS14;RPS27;RPL18A;RPL13;RPL27;RPL37;EIF3C;RPS10;RPL39;RPS12;RPS23
Selenocysteine synthesis	R-HSA-2408557	28	116	1.54E-05	8.14E-04	RPS9;RPL30;RPL21;RPS8;RPL34;RPL12;RPL35A;RPL23A;RPS3A;RPL3L;RPL7;RPS4X;RPS14;RPS27;RPL18A;RPL13;RPL27;RPL37;RPS10;RPL39;RPS12;RPS23
Adaptive Immune System	R-HSA-1280218	138	1002	2.18E-05	0.001	IGHV4;FBXO27;IGHV3-23;IGHV1-2;ICAM3;ITGAL;TREM1;IGLV4-60;ICAM1;IGLV2-8;TRIM9;PPP2R1B;ELOB;CD36;PRKG1;HLA-H;TRIM63;CD300A;HLA-B;HLA-C;HLA-A;BTN3A2;HLA-F;DNM3;RNF144B;PRKCQ;RAPGEF3;IGLV3-19;CLEC4G;HLA-DQB1;UBR4;RASGRP3;PSMB6;HLA-DMB;IGLV1-47;KLRC4-KLRK1;IGLV1-44;CD14;PAG1;HLA-DQA1;CAP2;DYNC1H1;HLA-DRB5;IGLC7;ERAP2;IGKV2D-40;ERAP1;LILRB2;CLEC2B;SELL;CD209;FCGR2B;HLA-DRB1;LGMN
Generation of second messenger molecules	R-HSA-202433	18	58	2.24E-05	0.001	HLA-DRB5;HLA-DQA1;HLA-DRB1;HLA-DQB1
SRP-dependent cotranslational protein targeting to membrane	R-HSA-1799339	28	121	3.19E-05	0.001	RPS9;RPL30;RPL21;RPS8;RPL34;RPL12;RPL35A;RPL23A;RPS3A;RPL3L;RPL7;RPS4X;RPS14;RPS27;RPL18A;RPL13;RPL27;RPL37;RPS10;RPL39;RPS12;RPS23
Nonsense-Mediated Decay (NMD)	R-HSA-927802	28	124	4.83E-05	0.002	RPS9;RPL30;RPL21;RPS8;RPL34;RPL12;RPL35A;RPL23A;RPS3A;RPL3L;RPL7;RPS4X;RPS14;RPS27;RPL18A;RPL13;RPL27;RPL37;RPS10;RPL39;RPS12;RPS23
Nonsense Mediated Decay (NMD) enhanced by the Exon Junction Complex (EJC)	R-HSA-975957	28	124	4.83E-05	0.002	RPS9;RPL30;RPL21;RPS8;RPL34;RPL12;RPL35A;RPL23A;RPS3A;RPL3L;RPL7;RPS4X;RPS14;RPS27;RPL18A;RPL13;RPL27;RPL37;RPS10;RPL39;RPS12;RPS23
Eukaryotic Translation Initiation	R-HSA-72613	29	131	5.04E-05	0.002	RPS9;RPL30;RPL21;RPS8;RPL34;RPL12;RPL35A;RPL23A;RPS3A;RPL3L;RPL7;RPS4X;RPS14;RPS27;RPL18A;EIF3CL;RPL13;RPL27;RPL37;EIF3C;RPS10;RPL39;RPS12;RPS23
Cap-dependent Translation Initiation	R-HSA-72737	29	131	5.04E-05	0.002	RPS9;RPL30;RPL21;RPS8;RPL34;RPL12;RPL35A;RPL23A;RPS3A;RPL3L;RPL7;RPS4X;RPS14;RPS27;RPL18A;EIF3CL;RPL13;RPL27;RPL37;EIF3C;RPS10;RPL39;RPS12;RPS23
Integrin cell surface interactions	R-HSA-216083	20	86	3.80E-04	0.015	VWF;ITGA1;TNC;FN1;ICAM3;ITGAL;F11R;HSPG2;THBS1;ICAM1;COL4A2;COL4A1;COL4A4;ITGA10;COL4A3;KDR;COL10A1;ITGA7;ITGB6;ITGA5
Interleukin-4 and 13 signaling	R-HSA-6785807	37	212	5.69E-04	0.022	LAMA5;CCL22;MMP1;MAOA;HGF;MMP3;FN1;F13A1;FGF2;ICAM1;IGHG1;CCND1;BCL6;IL1B;CCL2;RHOU;LBP;CD36
Major pathway of rRNA processing in the nucleolus and cytosol	R-HSA-6791226	33	189	0.001	0.041	RPL30;RPL34;RPL12;PWP2;RPL7;RRP7A;RPS4X;RPS14;RPL18A;RPL13;RPL37;RPS10;RPL39;RPS12;RPS9;RPL21;RPS8;RPL35A;RPL23A;RPS3A;DDX52;MPP6;RPL23;RPS27;RPL27;SKI;RPS23
Regulation of expression of SLITs and ROBOs	R-HSA-9010553	32	183	0.001	0.046	RPL30;RPL34;RPL12;RPL7;RPS4X;PSMB6;RPS14;RPL18A;RPL13;ELOB;LIT2;RPL37;RPS10;RPL39;RPS12;RPS9;RPL21;RPS8;RPL35A;RPL23A;RPS3A;RPL3L;RPS27;RPL27;RPS23
MET activates PTK2 signaling	R-HSA-8874081	10	32	0.001	0.048	LAMA5;LAMA2;COL24A1;LAMB3;LAMA1;HGF;FN1;LAMB1;LAMC2;LAMC1

Table 4.3 Reactome analysis resulted in 38 significantly enriched pathways.

CHAPTER 5: DISCUSSION AND FUTURE DIRECTIONS

5.1 SUMMARY

Even after successful treatment, breast cancer often leaves patients with a sense of identity loss and for these women, reconstructive surgery is a path to normalcy. [5,6] With improvements in the 5 and 10 year survival rates and increased screening for risk associated genes, the demand for breast reconstruction has increased 39% over the last 15 years. [3] The most common cause of revision in patients undergoing breast reconstruction is capsular contracture, a foreign body reaction that has a reported incidence between 1 and 50%. [7,12,15–17] In capsular contracture the scar tissue surrounding the implant contracts and distorts implant shape, and in some instances, causes pain.

A search for "breast capsular contracture" results in 14,700 articles, a vast body of knowledge. However, there is still a general lack of consensus on certain clinical variable's influence on capsule severity and mechanisms that differentiate mild and severe capsular contracture. The work presented here aims to lay a foundation for which of these lingering gaps can be addressed.

In Chapter 2 we presented a novel predictive model for capsule severity in patients undergoing reconstruction. The model was trained on clinical data from 89 patients and was able to reach an R^2 of 0.94 with only a 4.5% misclassification rate. With further validation, this model can be used to inform patients of their specific risk for severe capsular contracture and assist with patient education about lifestyle choices that could impact their reconstruction, such as smoking.

In Chapter 3 the use of a well-controlled clinical model, and new approaches to quantitative analysis, led to the discovery of novel attributes of capsule structure. By evaluating not only quantities of cells, but their distribution with respect to other capsule constituents, a new priming nexus of fibrosis was described. This region is the meeting of an M2 macrophage dense implant interface that is rich with collagen VI with an adjacent collagen III and I dense region populated with activated fibroblasts. These findings will further inform mechanistic inquiries of capsular contracture and could potentially lead to new treatment approaches.

In Chapter 4 RNA-seq was applied to the same controlled clinical model. This analysis provided unprecedented detail of the differential gene expression and enriched pathways found in severe capsular contracture. Between-patient variability proved a large contributor to differences in expression, so a paired analysis, utilizing samples from patients with asymmetric capsule grades, was performed. This method identified 1029 genes and 38 pathways that were significantly dysregulated. When validated these results can be used to better understand the driving pathways of capsule severity and explore novel drug targets to mitigate those pathways.

5.2 CHALLENGES, LIMITATIONS, AND FUTURE WORK

Cell isolation

This dissertation describes a plethora of observations that correlate to capsule severity; however it lacks mechanistic experiments, which are needed to move from observations to potential interventions. The work of Kyle et al demonstrated that capsule fibroblasts are different from fibroblasts from common sources, indicating that primary cells isolated from capsule tissue would be ideal for mechanistic studies.[38] The isolation of cells from capsule tissue proved challenging. Many protocols exist for isolating cells from fibrous tissue, but due to sample size, only tissue explant culture was feasible. This made the culture of immune cells unfeasible and focused isolation protocols on fibroblasts. It was soon discovered that clinical tissues were arriving at the lab with significant bacterial contamination that was resistant to standard culture antibiotics. Systematic testing of different aspects of the tissue's pipeline revealed that 'sterile' gauze that was added to the specimens in the operating room to maintain moisture was the source of contamination. Removing the gauze and using gentamicin as the culture antibiotic solved the contamination problems. The moisture retaining properties of the gauze were found to be unnecessary due to the relatively rapid time course of tissue processing. For patient samples, explant culture was not conducive to consistent culture lengths. Some explants grew out quickly and could be frozen down within two weeks, others failed to fill a 60mm plate after 1 month.

Freezing and standardization of cell numbers also proved difficult. Cells from different patients spread to different degrees so the confluent number of cells per p100 plate could vary by an order of magnitude. DMSO and serum concentrations in the freeze medium were evaluated by cell survival, but no one concentration was suitable for all samples tested. After reaching confluency

the first passage, cells were isolated, counted and frozen. The final protocol consisted of freezing half of a p100's cells in 1ml of DMEM glutamax with 10% fetal bovine serum and 10% DMSO. For those cells that could be frozen down, none had greater than 50% survival after defrosting and plating and many did not survive the freeze down process. No cell lines survived beyond passage 3, which limited the total number of cells that could be generated per sample, hindering cell culture experiments. Being unable to validate histological findings by cell assays has limited the amount of mechanistic data presented in this dissertation.

Single Time Point Study

The data presented here are all collected from a single time period in capsule development. No correlations to residing time were detected, however, temporal aspects of capsule development should not be ignored. To date, it is unclear if increased capsule severity is related to an increased rate of capsule formation. Said another way, if given sufficient time, would a grade I capsule eventually progress to a higher capsule grade? This study cannot answer that question. Further clinical data is being collected on the patients tracked in our study to follow their long term responses to their silicone implants. One year follow-up data has been collected for 10 patients, but the expander grade and implant grade do not show correlation within this small cohort. By continuing to collect follow up information, correlations may emerge once more patients are added or longer time points have been collected. Having collected detailed histology and expression data on these patients initial reaction to implants, places this study in a unique position going forward. It is possible the immune response to the expander is predictive of the 5 or 10 year reactions to silicone implants.

5.2.1 FUTURE WORK FOR NEURAL NETWORK MODEL

Expand Dataset for Training

Currently, the model is trained on roughly 80 patients and validated on 10. Ideally, the model would be trained on 10-fold as many patients. For instance, the number of patients with diabetes and smoking may be too small to detect an effect from those variables. Once sample size is increased, persistent misclassifications should be investigated in depth to identify potential causes of error. The current IRB does not allow for the additional collection of patient data beyond what is present in their medical history. More in-depth family histories may be necessary and some data may require additional testing on the patient, e.g., blood glucose curves, additional blood or tissue samples.

Future Clinical Experiments

Additional IRBs will be needed to obtain clinical correlates for capsule thickness and vessel size. With approval, patients can be screened with Doppler flow ultrasound at a high resolution at a series of time points, possibly at the same appointments used to increase expander volume. Data collection might also be continued out to one to five years post-implant placement. By doing so, the adaptability of the model's predictions to final silicone implants could be addressed. To date, it is unclear if the temporal development of vasculature is the same between expanders and silicone implants. If different, this data will inform the model adjustments necessary to predict capsule severity in permanent implants.

Expansion of Diabetes Variable

The current model represents diabetes as a binary variable and bins type I and II diabetes together for the positive condition. While this appears to be sufficient to predict capsule grade, it is not as useful for physicians. It would be ideal to show patients how controlling their blood sugar impacts their surgical outcomes. In order to add this capability, further data on blood sugar levels will need to be collected from both normal and diabetic patients at the time of surgery. It may be difficult to collect data on patients who undergo surgery with uncontrolled blood sugar because patients are normally asked to be within an acceptable range before being allowed to move forward with

surgery. It may be necessary to rely on the degree of variation between daily samples taken after surgery as a reference for general blood sugar control.

Nonetheless, it may still be valuable to gather data on blood sugar levels of everyone undergoing reconstruction to further elucidate the diabetes phenotype. It is currently unclear if blood sugar levels alone are the reason for poor surgical outcomes in patients with diabetes. Data on outcomes from type I and II diabetes, as well as controls with various blood sugar levels, would further the field as a whole in understanding how blood sugar correlates to reconstruction results.

User Interface development

The complete model can be exported in JAVA and a user interface can be overlaid so that physicians or patients can easily enter their relevant medical information and see concise predictive information. Further investigation is required, however, development for a phone app platform is a reasonable first target. Physician and patient feedback will be necessary to determine the final display. For example, it may not be necessary to provide predicted risk for all capsule grades. That maybe too much information for a patient thus "Risk of severe contracture" or Grade III probability alone could be displayed. It may also be necessary to have two "settings" for the user, one for physicians and another for patients, to accommodate the different information depths appropriate for each.

5.2.2 FUTURE WORK FROM CHAPTER 3

Western Blot Analysis of Tissue and Fibroblast Lysate

Immunofluorescence is best at showing localization not magnitude. Further work in needed to confirm the quantities of each protein of interest. To do, this Western blots can be run on proteins of interest (Figure 5.1) from either the total tissue lysate or isolated fibroblasts. Linear operating range must first be determined for each protein and staining protocol to avoid signal saturation (Figure 5.1A). Certain proteins run differently depending on the sample type (5.1B CCN1) or preparation (5.1C Collagen 6, requires less stringent detergent). Once findings from Chapter 3 are confirmed, Western blotting can also be used to evaluate pathways that influence proteins of interest and inform mechanistic studies.

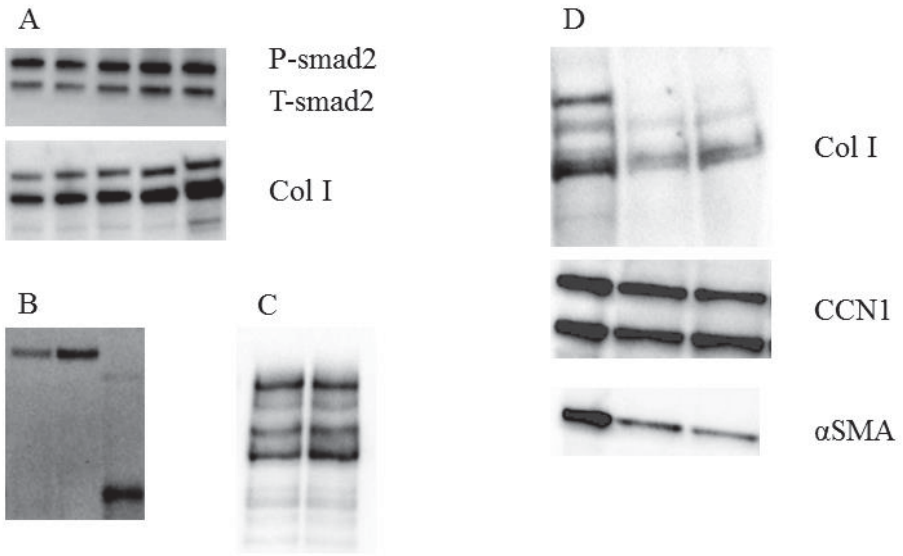

Figure 5.1. Optimization of Various Markers from tissue and cell lysates. A) Ranges of sample load can be tested for each protein to identify the linear detection range of the technique B) the first two lanes contain sample from patient tissue while the third is cell lysate, demonstrating that optimization is required for each sample type. C) Collagen VI required a different sample preparation than all other markers tested and was very sensitive to the amount and type of detergent used. D) When optimization is complete numerous markers can be probed on the same gel and normalized to total protein or a benchmark such as GAPDH.

An In Vitro/In Vivo Model of Capsule Formation

As acknowledged earlier, rodent models are not ideal for the clinical evaluation of capsular contracture; however, they are an excellent tool for basic science. Dr. Sarah Dallas has created mice with col1α2 tagged with GFP or mCherry at the University of Missouri Kansas City.[231] With the existence of such an animal one can begin to envision an experiment which could elaborate on numerous unanswered questions about fibroblasts presented in Chapter 3.

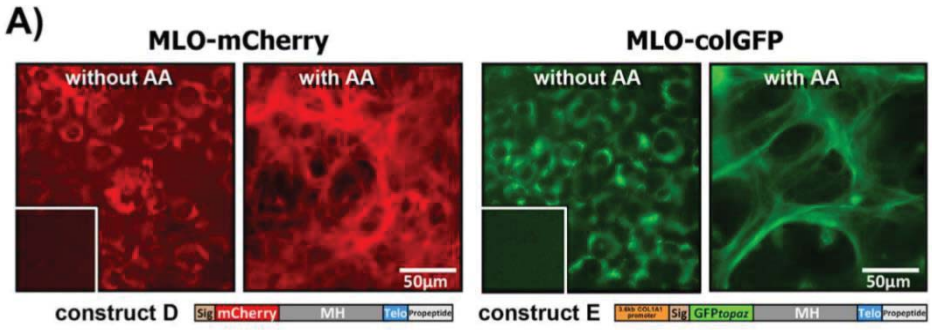

Figure 5.2 Reproduced from [232], fibroblasts expressing the mCherry and GFP constructs with and without the presence of ascorbic acid.

Most pertinent to this work, fibroblast collaboration in the healing matrix can be evaluated. Chapter 3 demonstrated the generation of subunits of maturity in the collagen matrix. One question concerning such discrete sectors is whether they are generated by clonally related populations of fibroblasts or cells that share less proximal mother cells. An initial approach to address this question, would be to co-culture fibroblasts producing either red or green collagen in an unlabeled collagen gel and imaged as they generate matrix. The gels could be fixed and stained afterwards for collagen I, allowing for the quantification of newly synthesized by each subpopulation vs reused collagen in the final gel. Another potential use for these animals is to look at contributions of different lineages of fibroblasts to given wound healing scenarios. A bone marrow transplant from a GFP mouse to an mCherry mouse would allow for the detection of collagen being produced from a bone marrow lineage (e.g. fibrocytes). Use of lineage tracing techniques, such as "brainbow" mice might also provide insight on relationships between and the behaviors of "scar-generating" cells.[233]

Fluorescence Activated Cell Sorting

The current study had limited patient material to work with, thus FACs was not possible. If larger tissue samples could be collected, macrophages and fibroblasts can be isolated directly from the tissue and placed in a variety of test conditions. In addition to a plethora of single cell type preparations, numerous co culture techniques could be implemented. One such model lends itself very nicely to addressing questions about the organization of interface region identified in the present study.[234] Two collagen gels can be produced, seeded with macrophages or fibroblasts, and then sandwiched together. Applying pressure forces out excess water and creates a thin, matrix dense gel that can be readily imaged.

With this base model in place, mechanistic inquiries might be made in a number of directions. Macrophages from a high-grade capsule could be paired with fibroblasts from a low-grade capsule or vice versa. Assays such as αSMA, caspase 3 activation, proliferation and cytokine production could help elucidate how the interface influences capsule structure and severity. Additionally, potential treatments could be tested in such a system for efficacy in preventing contraction.

5.2.3 FUTURE WORK FOR RNA-SEQ ANALYSIS

Before greater commitment is made to any one RNA-seq result, the data should first be further validated with qPCR and a protein analyses, either histological or Western blot analyses, to better determine the meaning of a significant (positive or negative) read count. For example, a high mRNA expression value may not translate to large amounts of a protein present and vice versa. Without a complete timeline of capsule formation, having protein and expression data for a given target is a good initial picture of what is occurring. An example of this method is seen in Figure 5.3. In the case of CYR61/ CCN1 expression was validated with qPCR and protein was quantified with immunofluorescence staining. For CCN1, expression appears to directly relate to protein quantity present in the tissue. The pattern suggests that expression has been higher in Grade III capsules for some period of time and continues to be increased at 4 months post-implantation. Western blots (not shown) suggest that CCN1 is strongly bound to other matrix components in tissue lysates, so co-immunoprecipitation with this protein may be enlightening.

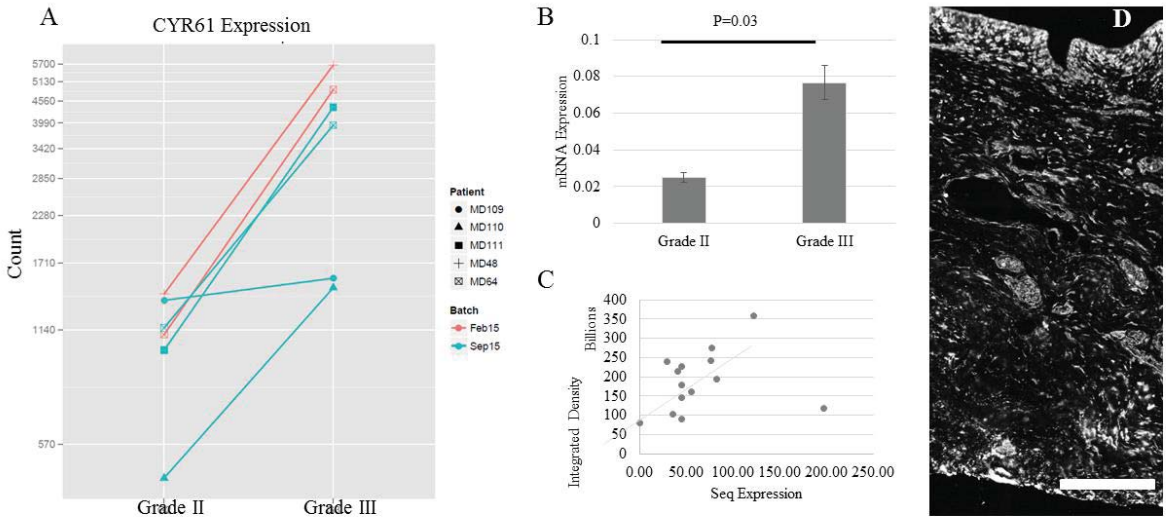

Figure 5.3. Validation of RNA-seq Identified Entity: CCN1 A) RNA-seq demonstrated a strong difference in CCN1 expression between capsule grades. B) These findings were confirmed with qPCR. D) The result was further validated with immunofluorescence staining for the protein and was found to be well correlated to the mRNA expression pattern (C).

REFERENCES

1. Ghose, T. Vintage Bling: Ancient Celts Had Shiny Dental Implants. *Live Science* (2014). at <http://www.livescience.com/46788-ancient-dental-implant-found.html>
2. Xia, Z. & Triffitt, J. T. A review on macrophage responses to biomaterials. *Biomed. Mater.* **1,** R1-9 (2006).
3. *2016 Plastic Surgery Statistics*. (2016). at <www.plasticsurgery.org>
4. Neuburger, J., Macneill, F., Jeevan, R., van der Meulen, J. H. P. & Cromwell, D. A. Trends in the use of bilateral mastectomy in England from 2002 to 2011: retrospective analysis of hospital episode statistics. *BMJ Open* **3,** e003179 (2013).
5. Lammer, C. *et al.* Sociology of breast tissue. *Eur. Surg.* **39,** 208–215 (2007).
6. Sandell, K. Stories without Significance in the Discourse of Breast Reconstruction. *Sci. Technol. Human Values* **33,** 326–344 (2008).
7. Thoma, A., Kaur, M., Waltho, D. & Bernice, T. in *Breast Reconstruction* (ed. Shiffman, M. A.) 481–499 (Springer International Publishing, 2016). doi:10.1007/978-3-319-18726-6
8. Nakazaki, T., Ikeda, K., Iwasaki, K. & Umezu, M. Regulatory science of new technology: tendency of medical professionals' interests on silicone breast implants. *J. Artif. Organs* (2016). doi:10.1007/s10047-016-0888-7
9. American Society of Plastic Surgeons. Breast Reconstruction Awareness Campaign. (2012). at <http://www.plasticsurgery.org/corporate-opportunities/corporate-support-opportunities/breast-reconstruction-awareness-campaign.html>
10. Gurunluoglu, R., Gurunluoglu, A., Williams, S. A. & Tebockhorst, S. Current trends in breast reconstruction: survey of American Society of Plastic Surgeons 2010. *Ann. Plast. Surg.* **70,** 103–10 (2013).
11. DeBoer, M., van der Hulst, R. & Slatman, J. The Surprise of a Breast Reconstruction: A Longitudinal Phenomenological Study to Women's Expectations About Reconstructive Surgery - The-surprise-of-a-breast-reconstruction.pdf. *Hum. Stud.* **38,** 409–430 (2015).
12. O'Shaughnessy, K. Evolution and update on current devices for prosthetic breast reconstruction. *Gland Surg.* **4,** 97–110 (2015).
13. Garusi, C. & Lohsiriwat, V. in *Oncoplastic and Reconstructive Breast Surgery* 315–320 (Springer International Publishing, 2013).

14. Ersek, R. A. Rate and incidence of capsular contracture: a comparison of smooth and textured silicone double-lumen breast prostheses. *Plast. Reconstr. Surg.* **87,** 879–84 (1991).
15. Asplund, O. Capsular contracture in silicone gel and saline-filled breast implants after reconstruction. *Plast. Reconstr. Surg.* **73,** 270–5 (1984).
16. Gylbert, L., Asplund, O. & Jurell, G. Capsular contracture after breast reconstruction with silicone-gel and saline-filled implants: a 6-year follow-up. *Plast. Reconstr. Surg.* **85,** 373–7 (1990).
17. Wong, C.-H., Samuel, M., Tan, B.-K. & Song, C. Capsular contracture in subglandular breast augmentation with textured versus smooth breast implants: a systematic review. *Plast. Reconstr. Surg.* **118,** 1224–36 (2006).
18. Spear, S. L. & Murphy, D. K. Natrelle round silicone breast implants: Core Study results at 10 years. *Plast. Reconstr. Surg.* **133,** 1354–61 (2014).
19. Prantl, L., Pöppl, N., Horvat, N., Heine, N. & Eisenmann-Klein, M. Serologic and histologic findings in patients with capsular contracture after breast augmentation with smooth silicone gel implants: is serum hyaluronan a potential predictor? *Aesthetic Plast. Surg.* **29,** 510–8 (2005).
20. Stevens, W. G. *et al.* Risk factor analysis for capsular contracture: a 5-year Sientra study analysis using round, smooth, and textured implants for breast augmentation. *Plast. Reconstr. Surg.* **132,** 1115–23 (2013).
21. Hvilsom, G. B. *et al.* Delayed breast implant reconstruction: is radiation therapy associated with capsular contracture or reoperations? *Ann. Plast. Surg.* **68,** 246–52 (2012).
22. Dancey, A., Nassimizadeh, A. & Levick, P. Capsular contracture - What are the risk factors? A 14 year series of 1400 consecutive augmentations. *J. Plast. Reconstr. Aesthet. Surg.* **65,** 213–8 (2012).
23. Nakhlis, F. *et al.* Abstract P6-18-02: Patterns of breast reconstruction in patients diagnosed with inflammatory breast cancer. *Cancer Res.* **76,** P6-18-02- (2016).
24. Wagner, R. *et al.* Abstract P2-13-02: Radiation and depression associated with complications of tissue expander reconstruction. *Cancer Res.* **76,** P2-13-02- (2016).
25. Tan, K. T., Wijeratne, D., Shih, B., Baildam, a D. & Bayat, a. Tumour necrosis factor-α expression is associated with increased severity of periprosthetic breast capsular

contracture. *Eur. Surg. Res.* **45,** 327–32 (2010).

26. Agnello, M. *et al.* Association of Microbial Growth on Silicone Breast Implants with Capsular Contracture: A Systematic Review. *J. Aesthetic Reconstr. Surg.* **1,** 1–5 (2015).
27. Ajdic, D., Zoghbi, Y., Gerth, D., Panthaki, Z. J. & Thaller, S. The Relationship of Bacterial Biofilms and Capsular Contracture in Breast Implants. *Aesthet. Surg. J.* **36,** 297–309 (2016).
28. Rieger, U. M. *et al.* Bacterial biofilms and capsular contracture in patients with breast implants. *Br. J. Surg.* **100,** 768–74 (2013).
29. Tamboto, H., Vickery, K. & Deva, A. K. Subclinical (biofilm) infection causes capsular contracture in a porcine model following augmentation mammaplasty. *Plast. Reconstr. Surg.* **126,** 835–42 (2010).
30. Hwang, K., Sim, H. B., Huan, F. & Kim, D. J. Myofibroblasts and capsular tissue tension in breast capsular contracture. *Aesthetic Plast. Surg.* **34,** 716–21 (2010).
31. Moyer, K. E. & Ehrlich, H. P. Capsular contracture after breast reconstruction: collagen fiber orientation and organization. *Plast. Reconstr. Surg.* **131,** 680–5 (2013).
32. Wolfram, D. *et al.* Cellular and molecular composition of fibrous capsules formed around silicone breast implants with special focus on local immune reactions. *J. Autoimmun.* **23,** 81–91 (2004).
33. Kyle, D. J. T. *et al.* Identification of molecular phenotypic descriptors of breast capsular contracture formation using informatics analysis of the whole genome transcriptome. *Wound Repair Regen.* **21,** 762–9 (2013).
34. Wolfram, D. *et al.* Cellular and molecular composition of fibrous capsules formed around silicone breast implants with special focus on local immune reactions. *J. Autoimmun.* **23,** 81–91 (2004).
35. Britez, M. E. M., Llano, C. C. & Chaux, A. Periprosthetic breast capsules and immunophenotypes of inflammatory cells. *Eur. J. Plast. Surg.* **35,** 647–651 (2012).
36. Sheng, L., Yu, Q., Xie, F. & Li, Q. Foreign body response induced by tissue expander implantation. *Mol. Med. Rep.* **9,** 872–6 (2014).
37. Wolfram, D. *et al.* T regulatory cells and TH17 cells in peri-silicone implant capsular fibrosis. *Plast. Reconstr. Surg.* **129,** 327e–337e (2012).
38. Kyle, D. J. T. & Bayat, A. Enhanced Contraction of a Normal Breast-Derived Fibroblast-

Populated Three-Dimensional Collagen Lattice via Contracted Capsule Fibroblast-Derived Paracrine Factors: Functional Significance in Capsular Contracture Formation. *Plast. Reconstr. Surg.* **135,** 1413–29 (2015).

39. Damanik, F. F. R., Rothuizen, T. C., van Blitterswijk, C., Rotmans, J. I. & Moroni, L. Towards an in vitro model mimicking the foreign body response: tailoring the surface properties of biomaterials to modulate extracellular matrix. *Sci. Rep.* **4,** 6325 (2014).
40. Bachhuka, A., Hayball, J., Smith, L. E. & Vasilev, K. E ff ect of Surface Chemical Functionalities on Collagen Deposition by Primary Human Dermal Fibroblasts. (2015). doi:10.1021/acsami.5b08249
41. Anderson, J. M., Rodriguez, A. & Chang, D. T. Foreign body reaction to biomaterials. *Semin. Immunol.* **20,** 86–100 (2008).
42. Luttikhuizen, D. T., Harmsen, M. C. & Van Luyn, M. J. A. Cellular and molecular dynamics in the foreign body reaction. *Tissue Eng.* **12,** 1955–70 (2006).
43. Higgins, D. M. *et al.* Localized immunosuppressive environment in the foreign body response to implanted biomaterials. *Am. J. Pathol.* **175,** 161–70 (2009).
44. Katzin, W. E., Feng, L. J., Abbuhl, M. & Klein, M. A. Phenotype of lymphocytes associated with the inflammatory reaction to silicone gel breast implants. *Clin. Diagn. Lab. Immunol.* **3,** 156–61 (1996).
45. Phillips, J. M. & Kao, W. J. Macrophage adhesion on gelatin-based interpenetrating networks grafted with PEGylated RGD. *Tissue Eng.* **11,** 964–73 (2005).
46. Parham, P. *The Immune System, 3rd Edition:* (Garland Science, 2009).
47. Stein, M., Keshav, S., Harris, N. & Gordon, S. Interleukin 4 potently enhances murine macrophage mannose receptor activity: a marker of alternative immunologic macrophage activation. *J. Exp. Med.* **176,** 287–92 (1992).
48. Martinez, F. O., Helming, L. & Gordon, S. Alternative activation of macrophages: an immunologic functional perspective. *Annu. Rev. Immunol.* **27,** 451–83 (2009).
49. Wilson, H., Barker, R. & Erwig, L.-P. Macrophages: Promising Targets for the Treatment of Atherosclerosis. *Curr. Vasc. Pharmacol.* **7,** 234–243 (2009).
50. Mosser, D. M. The many faces of macrophage activation. *J. Leukoc. Biol.* **73,** 209–212 (2003).
51. Song, E. *et al.* Influence of alternatively and classically activated macrophages on

fibrogenic activities of human fibroblasts. *Cell. Immunol.* **204,** 19–28 (2000).

52. Gordon, S. & Martinez, F. O. Alternative activation of macrophages: mechanism and functions. *Immunity* **32,** 593–604 (2010).
53. Sahin, E. *et al.* Macrophage PTEN regulates expression and secretion of arginase I modulating innate and adaptive immune responses. *J. Immunol.* **193,** 1717–27 (2014).
54. Stout, R. D. & Suttles, J. Functional plasticity of macrophages: reversible adaptation to changing microenvironments. *J. Leukoc. Biol.* **76,** 509–13 (2004).
55. Stout, R. D. & Suttles, J. Immunosenescence and macrophage functional plasticity: dysregulation of macrophage function by age-associated microenvironmental changes. *Immunol. Rev.* **205,** 60–71 (2005).
56. Arnold, L. *et al.* Inflammatory monocytes recruited after skeletal muscle injury switch into antiinflammatory macrophages to support myogenesis. *J. Exp. Med.* **204,** 1057–69 (2007).
57. Fantini, M. C. *et al.* IL-21 regulates experimental colitis by modulating the balance between Treg and Th17 cells. *Eur. J. Immunol.* **37,** 3155–63 (2007).
58. Niu, X. *et al.* IL-21 regulates Th17 cells in rheumatoid arthritis. *Hum. Immunol.* **71,** 334–41 (2010).
59. Pesce, J. *et al.* The IL-21 receptor augments Th2 effector function and alternative macrophage activation. *J. Clin. Invest.* **116,** 2044–55 (2006).
60. Barron, L. & Wynn, T. A. Fibrosis is regulated by Th2 and Th17 responses and by dynamic interactions between fibroblasts and macrophages. *Am. J. Physiol. Gastrointest. Liver Physiol.* **300,** G723-8 (2011).
61. ROSS, R. THE FIBROBLAST AND WOUND REPAIR. *Biol. Rev.* **43,** 51–91 (1968).
62. Direkze, N. C. *et al.* Multiple organ engraftment by bone-marrow-derived myofibroblasts and fibroblasts in bone-marrow-transplanted mice. *Stem Cells* **21,** 514–20 (2003).
63. Abe, R., Donnelly, S. C., Peng, T., Bucala, R. & Metz, C. N. Peripheral blood fibrocytes: differentiation pathway and migration to wound sites. *J. Immunol.* **166,** 7556–62 (2001).
64. Mori, L., Bellini, A., Stacey, M. A., Schmidt, M. & Mattoli, S. Fibrocytes contribute to the myofibroblast population in wounded skin and originate from the bone marrow. *Exp. Cell Res.* **304,** 81–90 (2005).
65. Higashiyama, R. *et al.* Differential contribution of dermal resident and bone marrow-

derived cells to collagen production during wound healing and fibrogenesis in mice. *J. Invest. Dermatol.* **131,** 529–36 (2011).

66. Barisic-Dujmovic, T., Boban, I. & Clark, S. H. Fibroblasts/myofibroblasts that participate in cutaneous wound healing are not derived from circulating progenitor cells. *J. Cell. Physiol.* **222,** 703–12 (2010).
67. Gabbiani, G., Ryan, G. B. & Majne, G. Presence of modified fibroblasts in granulation tissue and their possible role in wound contraction. *Experientia* **27,** 549–50 (1971).
68. Gabbiani, G. The biology of the myofibroblast. *Kidney Int.* **41,** 530–2 (1992).
69. Serini, G. & Gabbiani, G. Mechanisms of myofibroblast activity and phenotypic modulation. *Exp. Cell Res.* **250,** 273–83 (1999).
70. Ehrlich, H. P. Vanadate and the Absence of Myofibroblasts in Wound Contraction. *Arch. Surg.* **134,** 494–501 (1999).
71. Moyer, K. E., Davis, A., Saggers, G. C., Mackay, D. R. & Ehrlich, H. P. Wound healing: the role of gap junctional communication in rat granulation tissue maturation. *Exp. Mol. Pathol.* **72,** 10–6 (2002).
72. Lee, M. Y. & Ehrlich, H. P. Influence of vanadate on migrating fibroblast orientation within a fibrin matrix. *J. Cell. Physiol.* **217,** 72–6 (2008).
73. Au, K. & Ehrlich, H. P. When the Smad signaling pathway is impaired, fibroblasts advance open wound contraction. *Exp. Mol. Pathol.* **89,** 236–40 (2010).
74. Tomasek, J. J., Gabbiani, G., Hinz, B., Chaponnier, C. & Brown, R. a. Myofibroblasts and mechano-regulation of connective tissue remodelling. *Nat. Rev. Mol. Cell Biol.* **3,** 349–63 (2002).
75. Oliver, R. F. An autoradiographic study of 3H-thymidine incorporation and distribution in the dermis of healing skin incisions in the pig. *Br. J. Exp. Pathol.* **60,** 65–71 (1979).
76. McClain, S. A. *et al.* Mesenchymal cell activation is the rate-limiting step of granulation tissue induction. *Am. J. Pathol.* **149,** 1257–70 (1996).
77. Rørth, P. Collective guidance of collective cell migration. *Trends Cell Biol.* **17,** 575–9 (2007).
78. Ridley, A. J. *et al.* Cell migration: integrating signals from front to back. *Science* **302,** 1704–9 (2003).
79. DiMilla, P. A., Stone, J. A., Quinn, J. A., Albelda, S. M. & Lauffenburger, D. A. Maximal

migration of human smooth muscle cells on fibronectin and type IV collagen occurs at an intermediate attachment strength. *J. Cell Biol.* **122,** 729–37 (1993).

80. DiMilla, P. A., Quinn, J. A., Albelda, S. M. & Lauffenburger, D. A. Measurement of individual cell migration parameters for human tissue cells. *AIChE J.* **38,** 1092–1104 (1992).
81. Gaudet, C. *et al.* Influence of type I collagen surface density on fibroblast spreading, motility, and contractility. *Biophys. J.* **85,** 3329–35 (2003).
82. Welf, E. S., Ahmed, S., Johnson, H. E., Melvin, A. T. & Haugh, J. M. Migrating fibroblasts reorient directionality: By a metastable, PI3K-dependent mechanism. *J. Cell Biol.* **197,** 105–114 (2012).
83. Petrie, R. J., Doyle, A. D. & Yamada, K. M. Random versus directionally persistent cell migration. **10,** 538–549 (2010).
84. Doyle, A. D., Wang, F. W., Matsumoto, K. & Yamada, K. M. One-dimensional topography underlies three-dimensional fibrillar cell migration. *J. Cell Biol.* **184,** 481–90 (2009).
85. Even-Ram, S. & Yamada, K. M. Cell migration in 3D matrix. *Curr. Opin. Cell Biol.* **17,** 524–32 (2005).
86. Cukierman, E., Pankov, R., Stevens, D. R. & Yamada, K. M. Taking cell-matrix adhesions to the third dimension. *Science* **294,** 1708–1712 (2001).
87. Tamariz, E. & Grinnell, F. Modulation of fibroblast morphology and adhesion during collagen matrix remodeling. *Mol. Biol. Cell* **13,** 3915–29 (2002).
88. Chen, C. Z. & Raghunath, M. Focus on collagen: in vitro systems to study fibrogenesis and antifibrosis state of the art. *Fibrogenesis Tissue Repair* **2,** 7 (2009).
89. Liu, Y. *et al.* Control of cell migration in two and three dimensions using substrate morphology. *Exp. Cell Res.* **315,** 2544–57 (2009).
90. Häkkinen, L., Larjava, H. & Koivisto, L. in *Oral Wound Healing* (ed. Larjava, H.) (John Wiley & Sons, Ltd., 2012). doi:10.1002/9781118704509
91. Darby, I. A., Laverdet, B., Bonté, F. & Desmoulière, A. Fibroblasts and myofibroblasts in wound healing. *Clin. Cosmet. Investig. Dermatol.* **7,** 301–11 (2014).
92. Harris, A. K., Stopak, D. & Wild, P. Fibroblast traction as a mechanism for collagen morphogenesis. *Nature* **290,** 249–51 (1981).

93. Stopak, D., Wessells, N. K. & Harris, A. K. Morphogenetic rearrangement of injected collagen in developing chicken limb buds. *Proc. Natl. Acad. Sci. U. S. A.* **82,** 2804–8 (1985).
94. Gunn, J. S. & Ehrlich, H. P. Evidence that translocation of collagen fibril segments plays a role in early intrinsic tendon repair. *Plast. Reconstr. Surg.* **129,** 300e–306e (2012).
95. Meshel, A. S., Wei, Q., Adelstein, R. S. & Sheetz, M. P. Basic mechanism of three-dimensional collagen fibre transport by fibroblasts. *Nat. Cell Biol.* **7,** 157–64 (2005).
96. Giannone, G. *et al.* Periodic lamellipodial contractions correlate with rearward actin waves. *Cell* **116,** 431–43 (2004).
97. Castella, L. F., Buscemi, L., Godbout, C., Meister, J.-J. & Hinz, B. A new lock-step mechanism of matrix remodelling based on subcellular contractile events. *J. Cell Sci.* **123,** 1751–60 (2010).
98. Ehrlich, H. P. & Hunt, T. K. Collagen Organization Critical Role in Wound Contraction. *Adv. wound care* **1,** 3–9 (2012).
99. Welch, M. P., Odland, G. F. & Clark, R. A. Temporal relationships of F-actin bundle formation, collagen and fibronectin matrix assembly, and fibronectin receptor expression to wound contraction. *J. Cell Biol.* **110,** 133–45 (1990).
100. Canty, E. G. *et al.* Actin filaments are required for fibripositor-mediated collagen fibril alignment in tendon. *J. Biol. Chem.* **281,** 38592–38598 (2006).
101. Pelham, R. J. & Wang, Y. l. Cell locomotion and focal adhesions are regulated by substrate flexibility. *Proc. Natl. Acad. Sci. U. S. A.* **94,** 13661–5 (1997).
102. Rustad, K. C., Wong, V. W. & Gurtner, G. C. The role of focal adhesion complexes in fibroblast mechanotransduction during scar formation. *Differentiation.* **86,** 87–91 (2013).
103. Sheets, K., Wunsch, S., Ng, C. & Nain, A. S. Shape-dependent cell migration and focal adhesion organization on suspended and aligned nanofiber scaffolds. *Acta Biomater.* **9,** 7169–77 (2013).
104. Sharma, P., Sheets, K., Elankumaran, S. & Nain, A. S. The mechanistic influence of aligned nanofibers on cell shape, migration and blebbing dynamics of glioma cells. *Integr. Biol. (Camb).* **5,** 1036–44 (2013).
105. Sandbo, N. & Dulin, N. Actin cytoskeleton in myofibroblast differentiation: ultrastructure defining form and driving function. *Transl. Res.* **158,** 181–96 (2011).

106. Goffin, J. M. *et al.* Focal adhesion size controls tension-dependent recruitment of alpha-smooth muscle actin to stress fibers. *J. Cell Biol.* **172,** 259–68 (2006).
107. Werb, Z., Tremble, P. M., Behrendtsen, O., Crowley, E. & Damsky, C. H. Signal transduction through the fibronectin receptor induces collagenase and stromelysin gene expression. *J. Cell Biol.* **109,** 877–89 (1989).
108. Knox, P., Crooks, S. & Rimmer, C. S. Role of fibronectin in the migration of fibroblasts into plasma clots. *J. Cell Biol.* **102,** 2318–23 (1986).
109. Lareu, R. R., Arsianti, I., Subramhanya, H. K., Yanxian, P. & Raghunath, M. In vitro enhancement of collagen matrix formation and crosslinking for applications in tissue engineering: a preliminary study. *Tissue Eng.* **13,** 385–91 (2007).
110. McDonald, J. A., Kelley, D. G. & Broekelmann, T. J. Role of fibronectin in collagen deposition: Fab' to the gelatin-binding domain of fibronectin inhibits both fibronectin and collagen organization in fibroblast extracellular matrix. *J. Cell Biol.* **92,** 485–92 (1982).
111. Reyhani, V. *et al.* Fibrin binds to collagen and provides a bridge for αVβ3 integrin-dependent contraction of collagen gels. *Biochem. J.* **462,** 113–23 (2014).
112. Zimmerman, K. A., Graham, L. V, Pallero, M. A. & Murphy-Ullrich, J. E. Calreticulin regulates transforming growth factor-β-stimulated extracellular matrix production. *J. Biol. Chem.* **288,** 14584–98 (2013).
113. Van Duyn Graham, L., Sweetwyne, M. T., Pallero, M. A. & Murphy-Ullrich, J. E. Intracellular calreticulin regulates multiple steps in fibrillar collagen expression, trafficking, and processing into the extracellular matrix. *J. Biol. Chem.* **285,** 7067–78 (2010).
114. Mochida, Y. *et al.* Decorin modulates collagen matrix assembly and mineralization. *Matrix Biol.* **28,** 44–52 (2009).
115. Zhang, G. *et al.* Decorin regulates assembly of collagen fibrils and acquisition of biomechanical properties during tendon development. *J. Cell. Biochem.* **98,** 1436–49 (2006).
116. Schultz-Cherry, S. *et al.* Regulation of transforming growth factor-beta activation by discrete sequences of thrombospondin 1. *J. Biol. Chem.* **270,** 7304–10 (1995).
117. Subramanian, A. & Schilling, T. F. Thrombospondin-4 controls matrix assembly during development and repair of myotendinous junctions. *Elife* **2014,** 1–21 (2014).

118. Bradshaw, A. D. The role of secreted protein acidic and rich in cysteine (SPARC) in cardiac repair and fibrosis: Does expression of SPARC by macrophages influence outcomes? *J. Mol. Cell. Cardiol.* (2015). doi:10.1016/j.yjmcc.2015.11.014
119. Harris, B. S. *et al.* SPARC regulates collagen interaction with cardiac fibroblast cell surfaces. *Am. J. Physiol. Heart Circ. Physiol.* **301,** H841-7 (2011).
120. Bradshaw, A. D. The role of SPARC in extracellular matrix assembly. *J. Cell Commun. Signal.* **3,** 239–246 (2009).
121. Joseph, J., Mohanty, M. & Mohanan, P. V. Role of immune cells and inflammatory cytokines in regulation of fibrosis around silicone expander implants. *J. Mater. Sci. Mater. Med.* **21,** 1665–76 (2010).
122. Brown, J. J. & Bayat, A. Genetic susceptibility to raised dermal scarring. *Br. J. Dermatol.* **161,** 8–18 (2009).
123. Bayat, A., Bock, O., Mrowietz, U., Ollier, W. E. R. & Ferguson, M. W. J. Genetic susceptibility to keloid disease and hypertrophic scarring: transforming growth factor beta1 common polymorphisms and plasma levels. *Plast. Reconstr. Surg.* **111,** 535-43–6 (2003).
124. Spear, S. L. & Baker, J. L. Classification of capsular contracture after prosthetic breast reconstruction. *Plast. Reconstr. Surg.* **96,** 1119–23; discussion 1124 (1995).
125. Pu, Y., Mao, T.-C., Zhang, Y.-M., Wang, S. & Fan, D.-L. The role of postmastectomy radiation therapy in patients with immediate prosthetic breast reconstruction. *Medicine (Baltimore).* **97,** e9548 (2018).
126. Dayhoff, J. E. & DeLeo, J. M. Artificial neural networks. *Cancer* **91,** 1615–1635 (2001).
127. Hopfield, J. J. Artificial neural networks. *IEEE Circuits Devices Mag.* **4,** 3–10 (1988).
128. Eftekhar, B., Mohammad, K., Ardebili, H. E., Ghodsi, M. & Ketabchi, E. Comparison of artificial neural network and logistic regression models for prediction of mortality in head trauma based on initial clinical data. *BMC Med. Inform. Decis. Mak.* **5,** 3 (2005).
129. Price, R. K. *et al.* Applying artificial neural network models to clinical decision making. *Psychol. Assess.* **12,** 40–51 (2000).
130. Prantl, L. *et al.* Clinical and morphological conditions in capsular contracture formed around silicone breast implants. *Plast. Reconstr. Surg.* **120,** 275–84 (2007).
131. Bui, J. M. *et al.* Histological Characterization of Human Breast Implant Capsules.

Aesthetic Plast. Surg. **39,** 306–315 (2015).

132. Coleman, D. J., Sharpe, D. T., Naylor, I. L., Chander, C. L. & Cross, S. E. The role of the contractile fibroblast in the capsules around tissue expanders and implants. *Br. J. Plast. Surg.* **46,** 547–56 (1993).
133. Adkinson, J. M., Miller, N. F., Eid, S. M., Miles, M. G. & Murphy, R. X. Tissue Expander Complications Predict Permanent Implant Complications and Failure of Breast Reconstruction. *Ann. Plast. Surg.* (2014). doi:10.1097/SAP.0000000000000142
134. Seyhan, H. *et al.* Smooth and textured silicone surfaces of modified gel mammary prostheses cause a different impact on fibroproliferative properties of dermal fibroblasts. *J. Plast. Reconstr. Aesthet. Surg.* **64,** e60-6 (2011).
135. Boháč, M. *et al.* Histological and immunohistochemical characteristics of capsular synovial metaplasias that form around silicone breast implants. *Biologia (Bratisl).* 1–6 (2018). doi:10.2478/s11756-018-0024-7
136. Katzel, E. B. *et al.* A novel animal model for studying silicone gel-related capsular contracture. *Plast. Reconstr. Surg.* **126,** 1483–91 (2010).
137. Jacobson, L. K., Johnson, M. B., Dedhia, R. D., Niknam-Bienia, S. & Wong, A. K. Impaired wound healing after radiation therapy: A systematic review of pathogenesis and treatment. *JPRAS Open* **13,** 92–105 (2017).
138. Xu, Z. & Taylor, J. A. Genome-wide age-related DNA methylation changes in blood and other tissues relate to histone modification, expression and cancer. *Carcinogenesis* **35,** 356–364 (2014).
139. Giovannucci, E. *et al.* Diabetes and cancer: a consensus report. *Diabetes Care* **33,** 1674–85 (2010).
140. White, M. C. *et al.* Age and cancer risk: a potentially modifiable relationship. *Am. J. Prev. Med.* **46,** S7-15 (2014).
141. National Cancer Institute. Risk Factors: Age - National Cancer Institute. (2015). at <https://www.cancer.gov/about-cancer/causes-prevention/risk/age>
142. Guo, S. & Dipietro, L. A. Factors affecting wound healing. *J. Dent. Res.* **89,** 219–29 (2010).
143. Example of Predictor Screening. *JMP 13.2 Online Documentation* (2017). at <https://www.jmp.com/support/help/13-

2/Example_of_Predictor_Screening.shtml#494473>

144. Blount, A. L., Martin, M. D., Lineberry, K. D., Kettaneh, N. & Alfonso, D. R. Capsular contracture rate in a low-risk population after primary augmentation mammaplasty. *Aesthet. Surg. J.* **33,** 516–21 (2013).
145. Dirgenali, F. & Kara, S. Recognition of early phase of atherosclerosis using principles component analysis and artificial neural networks from carotid artery Doppler signals. *Expert Syst. Appl.* **31,** 643–651 (2006).
146. Oh, E.-T. *et al.* Radiation-induced angiogenic signaling pathway in endothelial cells obtained from normal and cancer tissue of human breast. *Oncogene* **33,** 1229–1238 (2014).
147. Hidalgo, D. a. Discussion: risk factor analysis for capsular contracture: a 5-year Sientra study analysis using round, smooth, and textured implants for breast augmentation. *Plast. Reconstr. Surg.* **132,** 1124–5 (2013).
148. Chuba, P. J. *et al.* Radiation and depression associated with complications of tissue expander reconstruction. *Breast Cancer Res. Treat.* 1–7 (2017). doi:10.1007/s10549-017-4277-6
149. Prantl, L. *et al.* Semiquantitative measurements of capsular contracture with elastography - First results in correlation to Baker Score. *Clin. Hemorheol. Microcirc.* (2014). doi:10.3233/CH-141812
150. Butterfly iQ - Whole body imaging, under $2k. at <https://www.butterflynetwork.com/>
151. Health, C. O. on S. and. Smoking and Tobacco Use; Fact Sheet. at <https://www.cdc.gov/tobacco/data_statistics/fact_sheets/index.htm>
152. Centers for Disease Control. National Diabetes Statistics Report, 2017 Estimates of Diabetes and Its Burden in the United States Background. (2017). at <https://www.cdc.gov/diabetes/pdfs/data/statistics/national-diabetes-statistics-report.pdf>
153. Ayoub, Z. *et al.* A 10-Year Experience with Mastectomy and Tissue Expander Placement to Facilitate Subsequent Radiation and Reconstruction. *Ann. Surg. Oncol.* 1–7 (2017). doi:10.1245/s10434-017-5956-6
154. Breast Cancer: Statistics | Cancer.Net. *Cancer.Net* (2017). at <https://www.cancer.net/cancer-types/breast-cancer/statistics>
155. Siani, A. & Tirelli, N. Myofibroblast differentiation: main features, biomedical relevance,

and the role of reactive oxygen species. *Antioxid. Redox Signal.* **21,** 768–85 (2014).

156. Van Linthout, S., Miteva, K. & Tschope, C. Crosstalk between fibroblasts and inflammatory cells. *Cardiovasc. Res.* **102,** 258–269 (2014).
157. Ploeger, D. T. *et al.* Cell plasticity in wound healing: paracrine factors of M1/ M2 polarized macrophages influence the phenotypical state of dermal fibroblasts. *Cell Commun. Signal.* **11,** 29 (2013).
158. Rich, L. & Whittaker, P. Collagen and Picrosirius Red Staining : a Polarized Light Assessment of Fibrillar Hue and Spatial Distribution. *Braz J Morphol Sci* **22,** 97–104 (2005).
159. Junqueira, L. C., Bignolas, G. & Brentani, R. R. Picrosirius staining plus polarization microscopy, a specific method for collagen detection in tissue sections. *Histochem. J.* **11,** 447–55 (1979).
160. Lattouf, R. *et al.* Picrosirius red staining: a useful tool to appraise collagen networks in normal and pathological tissues. *J. Histochem. Cytochem.* **62,** 751–8 (2014).
161. Degen, K. E. & Gourdie, R. G. Embryonic wound healing: A primer for engineering novel therapies for tissue repair. *Birth Defects Res. Part C - Embryo Today Rev.* **96,** 258–270 (2012).
162. Theocharidis, G. *et al.* Type VI Collagen Regulates Dermal Matrix Assembly and Fibroblast Motility. *J. Invest. Dermatol.* **136,** 74–83 (2015).
163. Lau, L. F. CCN1/CYR61: the very model of a modern matricellular protein. *Cell. Mol. Life Sci.* **68,** 3149–3163 (2011).
164. Jun, J.-I. & Lau, L. F. The matricellular protein CCN1 induces fibroblast senescence and restricts fibrosis in cutaneous wound healing. *Nat. Cell Biol.* **12,** 676–85 (2010).
165. Borkham-Kamphorst, E. *et al.* The anti-fibrotic effects of CCN1/CYR61 in primary portal myofibroblasts are mediated through induction of reactive oxygen species resulting in cellular senescence, apoptosis and attenuated TGF-β signaling. *Biochim. Biophys. Acta - Mol. Cell Res.* **1843,** 902–914 (2014).
166. Braga, T. T., Agudelo, J. S. H. & Camara, N. O. S. Macrophages during the fibrotic process: M2 as friend and foe. *Frontiers in Immunology* **6,** (2015).
167. Wolf, M. T., Vodovotz, Y., Tottey, S., Brown, B. N. & Badylak, S. F. Predicting In Vivo Responses to Biomaterials via Combined In Vitro and In Silico Analysis. *Tissue Eng. Part*

C. Methods **0,** 1–12 (2014).

168. Bernard, K. *et al.* Metabolic Reprogramming Is Required for Myofibroblast Contractility and Differentiation. *J. Biol. Chem.* **290,** 25427–38 (2015).
169. Kyle, D. J. T. & Bayat, A. Enhanced Contraction of a Normal Breast-Derived Fibroblast–Populated Three-Dimensional Collagen Lattice via Contracted Capsule Fibroblast-Derived Paracrine Factors. *Plast. Reconstr. Surg.* **135,** 1413–1429 (2015).
170. Hannan, R. T., Peirce, S. M. & Barker, T. H. Fibroblasts: Diverse Cells Critical to Biomaterials Integration. *ACS Biomater. Sci. Eng.* acsbiomaterials.7b00244 (2017). doi:10.1021/acsbiomaterials.7b00244
171. Grieb, G. *et al.* in *Burns & Trauma 2017 5:1* **5,** 1–19 (BioMed Central, 2011).
172. Humphreys, B. D. *et al.* Fate tracing reveals the pericyte and not epithelial origin of myofibroblasts in kidney fibrosis. *Am. J. Pathol.* **176,** 85–97 (2010).
173. Liu, S., Taghavi, R. & Leask, A. Connective tissue growth factor is induced in bleomycin-induced skin scleroderma. *J. Cell Commun. Signal.* **4,** 25–30 (2010).
174. Lin, S.-L., Kisseleva, T., Brenner, D. A. & Duffield, J. S. Pericytes and perivascular fibroblasts are the primary source of collagen-producing cells in obstructive fibrosis of the kidney. *Am. J. Pathol.* **173,** 1617–27 (2008).
175. Koumas, L., Smith, T. J., Feldon, S., Blumberg, N. & Phipps, R. P. Thy-1 Expression in Human Fibroblast Subsets Defines Myofibroblastic or Lipofibroblastic Phenotypes. *Am. J. Pathol.* **163,** 1291–1300 (2003).
176. Sanders, Y. Y. *et al.* Thy-1 Promoter Hypermethylation. *Am. J. Respir. Cell Mol. Biol.* **39,** 610–618 (2008).
177. Fernando, M. R., Giembycz, M. A. & McKay, D. M. Bidirectional crosstalk via IL-6, PGE_2 and PGD_2 between murine myofibroblasts and alternatively activated macrophages enhances anti-inflammatory phenotype in both cells. *Br. J. Pharmacol.* **173,** 899–912 (2016).
178. Gordon, S. Alternative activation of macrophages. *Nat. Rev. Immunol.* **3,** 23–35 (2003).
179. Van Putten ⇑, S. M., Ploeger, D. T. A., Popa, E. R. & Bank, R. A. Macrophage phenotypes in the collagen-induced foreign body reaction in rats. (2013). doi:10.1016/j.actbio.2013.01.022
180. Fabriek, B. O., Dijkstra, C. D. & van den Berg, T. K. The macrophage scavenger receptor

CD163. *Immunobiology* **210,** 153–160 (2005).

181. Jablonski, K. A. *et al.* Novel Markers to Delineate Murine M1 and M2 Macrophages. *PLoS One* **10,** e0145342 (2015).
182. Gensel, J. C., Kopper, T. J., Zhang, B., Orr, M. B. & Bailey, W. M. Predictive screening of M1 and M2 macrophages reveals the immunomodulatory effectiveness of post spinal cord injury azithromycin treatment. *Sci. Rep.* **7,** 40144 (2017).
183. Schnoor, M. *et al.* Production of Type VI Collagen by Human Macrophages: A New Dimension in Macrophage Functional Heterogeneity 1,2. at <http://macrophages.de/pubs/papers/J_Immunol_2008_180-8_5707-5719.pdf>
184. Naugle, J. E. *et al.* Type VI collagen induces cardiac myofibroblast differentiation: implications for postinfarction remodeling. *Am. J. Physiol. Heart Circ. Physiol.* **290,** H323-30 (2006).
185. Adams, W. P. *et al.* A rabbit model for capsular contracture: development and clinical implications. *Plast. Reconstr. Surg.* **117,** 1214-9–1 (2006).
186. Shin, K. C. *et al.* The effect of antiadhesion agent on peri-implant capsular formation in rabbits. *Ann. Plast. Surg.* **71,** 600–4 (2013).
187. Laitung, J. K., McClure, J. & Shuttleworth, C. A. The fibrous capsules around static and dynamic implants: their biochemical, histological, and ultrastructural characteristics. *Ann. Plast. Surg.* **19,** 208–16 (1987).
188. Antony, A. K., McCarthy, C., Disa, J. J. & Mehrara, B. J. Bilateral implant breast reconstruction: outcomes, predictors, and matched cohort analysis in 730 2-stage breast reconstructions over 10 years. *Ann. Plast. Surg.* **72,** 625–30 (2014).
189. Calobrace, M. B. *et al.* Risk Factor Analysis for Capsular Contracture. *Plast. Reconstr. Surg.* **141,** 20S–28S (2018).
190. Axillary Lymphadenectomy and Wound Complications in Implant-Based Breast Reconstruction. *Ann. Plast. Surg.*
191. Ricci, J. A. *et al.* A meta-analysis of implant-based breast reconstruction and timing of adjuvant radiation therapy. *J. Surg. Res.* **218,** 108–116 (2017).
192. Siggelkow, W. *et al.* Histological analysis of silicone breast implant capsules and correlation with capsular contracture. *Biomaterials* **24,** 1101–9 (2003).
193. Liu, X. *et al.* Comparison of the Postoperative Incidence Rate of Capsular Contracture

among Different Breast Implants: A Cumulative Meta-Analysis. *PLoS One* **10,** e0116071 (2015).

194. Kyle, D. J. T., Oikonomou, A., Hill, E. & Bayat, A. Development and functional evaluation of biomimetic silicone surfaces with hierarchical micro/nano-topographical features demonstrates favourable invitro foreign body response of breast-derived fibroblasts. *Biomaterials* **52,** 88–102 (2015).
195. Mortazavi, A., Williams, B. a, McCue, K., Schaeffer, L. & Wold, B. Mapping and quantifying mammalian transcriptomes by RNA-Seq. *Nat. Methods* **5,** 621–628 (2008).
196. Robles, J. A. *et al.* Efficient experimental design and analysis strategies for the detection of differential expression using RNA-Sequencing. *BMC Genomics* **13,** 484 (2012).
197. Marguerat, S. & Bähler, J. RNA-seq: from technology to biology. *Cell. Mol. Life Sci.* **67,** 569–579 (2010).
198. Hong, M.-G., Pawitan, Y., Magnusson, P. K. E. & Prince, J. A. Strategies and issues in the detection of pathway enrichment in genome-wide association studies. *Hum. Genet.* **126,** 289–301 (2009).
199. Liu, W. *et al.* Identification of Key Modules and Hub Genes of Keloids with Weighted Gene Coexpression Network Analysis. *Plast. Reconstr. Surg.* **2,** 376–390 (2017).
200. Croft, D. *et al.* Reactome: a database of reactions, pathways and biological processes. *Nucleic Acids Res.* **39,** D691–D697 (2011).
201. Aronesty, E. Comparison of Sequencing Utility Programs. *Open Bioinforma. J.* **7,** 1–8 (2013).
202. Kong, Y. Btrim: A fast, lightweight adapter and quality trimming program for next-generation sequencing technologies. *Genomics* **98,** 152–153 (2011).
203. Langmead, B. & Salzberg, S. L. Fast gapped-read alignment with Bowtie 2. *Nat. Methods* **9,** 357–359 (2012).
204. Anders, S., Pyl, P. T. & Huber, W. HTSeq--a Python framework to work with high-throughput sequencing data. *Bioinformatics* **31,** 166–9 (2015).
205. Love, M. I., Huber, W. & Anders, S. Moderated estimation of fold change and dispersion for RNA-seq data with DESeq2. *Genome Biol.* **15,** 550 (2014).
206. Haw, R., Hermjakob, H., D'Eustachio, P. & Stein, L. Reactome pathway analysis to enrich biological discovery in proteomics data sets. *Proteomics* **11,** 3598–3613 (2011).

207. Wassell, J. Haptoglobin: function and polymorphism. *Clin. Lab.* **46,** 547–52 (2000).
208. Smeets, M. B., Fontijn, J., Kavelaars, A., Pasterkamp, G. & De Kleijn, D. P. V. The acute phase protein haptoglobin is locally expressed in arthritic and oncological tissues. *Int. J. Exp. Pathol.* **84,** 69–74 (2003).
209. Luan, A. *et al.* Noncoding RNAs in Wound Healing: A New and Vast Frontier. *Adv. wound care* **7,** 19–27 (2018).
210. Li, J. *et al.* The Long Non-Coding RNA LncRNA8975-1 is Upregulated in Hypertrophic Scar Fibroblasts and Controls Collagen Expression. *Cell. Physiol. Biochem.* **40,** 326–334 (2016).
211. Chen, L. *et al.* Non-Coding RNAs: The New Insight on Hypertrophic Scar. *J. Cell. Biochem.* **118,** 1965–1968 (2017).
212. Peters, V. A., Joesting, J. J. & Freund, G. G. IL-1 receptor 2 (IL-1R2) and its role in immune regulation. *Brain. Behav. Immun.* **32,** 1–8 (2013).
213. Brown, D., Trowsdale, J. & Allen, R. The LILR family: modulators of innate and adaptive immune pathways in health and disease. *Tissue Antigens* **64,** 215–225 (2004).
214. UniProtKB-P10914. *Unitprot.org* (2018). at <https://www.uniprot.org/uniprot/P10914>
215. Jarosinski, K. W. & Massa, P. T. Interferon regulatory factor-1 is required for interferon-gamma-induced MHC class I genes in astrocytes. *J. Neuroimmunol.* **122,** 74–84 (2002).
216. Maruyama, S. *et al.* A novel function of interferon regulatory factor-1: inhibition of Th2 cells by down-regulating the Il4 gene during Listeria infection. *Int. Immunol.* **27,** 143–152 (2015).
217. Hobart, M., Ramassar, V., Goes, N., Urmson, J. & Halloran, P. F. IFN regulatory factor-1 plays a central role in the regulation of the expression of class I and II MHC genes in vivo. *J. Immunol.* **158,** 4260–9 (1997).
218. UNIProtKB-Q9Y6K5. *uniprot.org* (2018). at <https://www.uniprot.org/uniprot/Q9Y6K5>
219. Sheikh, Z., Brooks, P., Barzilay, O., Fine, N. & Glogauer, M. Macrophages, Foreign Body Giant Cells and Their Response to Implantable Biomaterials. *Materials (Basel).* **8,** 5671–5701 (2015).
220. Tsuruoka, N. *et al.* Bcl6 is required for the IL-4-mediated rescue of the B cells from apoptosis induced by IL-21. *Immunol. Lett.* **110,** 145–151 (2007).
221. Nurieva, R. I. *et al.* Bcl6 mediates the development of T follicular helper cells. *Science*

325, 1001–5 (2009).

222. Hatzi, K. *et al.* BCL6 orchestrates Tfh cell differentiation via multiple distinct mechanisms. *J. Exp. Med.* **212,** 539–53 (2015).

223. Liu, X. *et al.* Bcl6 expression specifies the T follicular helper cell program in vivo. *J. Exp. Med.* **209,** 1841–52, S1-24 (2012).

224. Chtanova, T. *et al.* T follicular helper cells express a distinctive transcriptional profile, reflecting their role as non-Th1/Th2 effector cells that provide help for B cells. *J. Immunol.* **173,** 68–78 (2004).

225. Scott, L. M., Civin, C. I., Rorth, P. & Friedman, A. D. A novel temporal expression pattern of three C/EBP family members in differentiating myelomonocytic cells. *Blood* **80,** 1725–35 (1992).

226. Choy, L. & Derynck, R. Transforming Growth Factor-β Inhibits Adipocyte Differentiation by Smad3 Interacting with CCAAT/Enhancer-binding Protein (C/EBP) and Repressing C/EBP Transactivation Function. *J. Biol. Chem.* **278,** 9609–9619 (2003).

227. Gery, S., Tanosaki, S., Hofmann, W.-K., Koppel, A. & Koeffler, H. P. C/EBPδ expression in a BCR-ABL-positive cell line induces growth arrest and myeloid differentiation. *Oncogene* **24,** 1589–1597 (2005).

228. Chen, Y.-T. *et al.* HDGF supports anti-apoptosis and pro-fibrosis in pancreatic stellate cells of pancreatic cancer. *bioRxiv* 272542 (2018). doi:10.1101/272542

229. Duitman, J. *et al.* CCAAT-enhancer binding protein delta (C/EBPδ) attenuates tubular injury and tubulointerstitial fibrogenesis during chronic obstructive nephropathy. *Lab. Investig.* **94,** 89–97 (2014).

230. Lin, J. *et al.* Cyr61 Induces IL-6 Production by Fibroblast-like Synoviocytes Promoting Th17 Differentiation in Rheumatoid Arthritis. *J. Immunol.* **188,** 5776–5784 (2012).

231. Kamel-ElSayed, S. A., Tiede-Lewis, L. M., Lu, Y., Veno, P. A. & Dallas, S. L. Novel approaches for two and three dimensional multiplexed imaging of osteocytes. *Bone* **76,** 129–40 (2015).

232. Lu, Y. *et al.* Live Imaging of Type I Collagen Assembly Dynamics in Osteoblasts Stably Expressing GFP and mCherry-tagged Collagen Constructs. *J. Bone Miner. Res.* (2018). doi:10.1002/jbmr.3409

233. Weissman, T. A. & Pan, Y. A. Brainbow: New Resources and Emerging Biological

Applications for Multicolor Genetic Labeling and Analysis. *Genetics* **199,** 293–306 (2015).

234. Kim, A., Lakshman, N., Karamichos, D. & Petroll, W. M. Growth Factor Regulation of Corneal Keratocyte Differentiation and Migration in Compressed Collagen Matrices. *Investig. Opthalmology Vis. Sci.* **51,** 864 (2010).